

# In vitro development and regeneration of primary cortical cell cultures of the grey short-tailed opossum *Monodelphis domestica*

---

**Mogorović, Sara**

**Master's thesis / Diplomski rad**

**2022**

*Degree Grantor / Ustanova koja je dodijelila akademski / stručni stupanj:* **University of Rijeka / Sveučilište u Rijeci**

*Permanent link / Trajna poveznica:* <https://um.nsk.hr/um:nbn:hr:193:544591>

*Rights / Prava:* [In copyright](#) / [Zaštićeno autorskim pravom.](#)

*Download date / Datum preuzimanja:* **2024-05-27**

*Repository / Repozitorij:*



[Repository of the University of Rijeka, Faculty of Biotechnology and Drug Development - BIOTECHRI Repository](#)



**UNIVERSITY OF RIJEKA**

**DEPARTMENT OF BIOTECHNOLOGY**

**Master's program**

**Drug Development and Research**

Sara Mogorović

***In vitro* development and regeneration of primary cortical cell  
cultures of the grey short-tailed opossum *Monodelphis domestica***

Master's thesis

Rijeka, 2022

UNIVERSITY OF RIJEKA  
DEPARTMENT OF BIOTECHNOLOGY  
Master's program  
Drug Development and Research

Sara Mogorović

***In vitro* development and regeneration of primary cortical cell  
cultures of the grey short-tailed opossum *Monodelphis domestica***

Master's thesis

Rijeka, 2022

Mentor: Assoc. Prof. Jelena Ban, PhD,

SVEUČILIŠTE U RIJECI

ODJEL ZA BIOTEHNOLOGIJU

Diplomski sveučilišni studij

Istraživanje i razvoj lijekova

Sara Mogorović

***In vitro* razvoj i regeneracija primarnih staničnih kultura  
korteksa oposuma *Monodelphis domestica***

Diplomski rad

Rijeka, 2022.

Mentor rada: izv. prof. dr. sc. Jelena Ban

## ***Acknowledgments***

I would like to sincerely thank Assoc. Prof. Jelena Ban for giving me the opportunity to be under her mentorship during my work in the laboratory, and most importantly, for her devoted time in guiding me through my Master's Thesis. I would also like to thank everyone in the Laboratory for Molecular Neurobiology who guided me through and wish them the best of luck in their future careers. I would also like to thank to all my biotechnology colleagues who I've met along my studies, who not only guided me and eased my studies, but also filled my days in Rijeka with joy and good spirit.

Most importantly, I am immensely grateful for Iva, Klara, Marina, Oton and Toni. Student life with you was a delight, and never with a dull moment. Thank you for everything you provided me with, your knowledge, your compassion, your brightness, your patience and most importantly, your love. You helped me shape into the person that I am today and allowed me to be my true self. I will cherish my time spent with you forever.

Cheers to our future journeys.

I would like to thank my family for always having my back, patience, and support through my academic and life choices.

To our little Sofia, you're the light of our lives, and I can't wait to see you grow and your interest spark.

Master's thesis was defended on 26<sup>th</sup> September, 2022

in front of the committee:

1. Prof. Miranda Mladinić Pejatović
2. Assist. Prof. Nicholas J. Bradshaw
3. Assoc. Prof. Jelena Ban

This thesis has 61 pages, 22 figures, 3 tables, and 50 references.

## ABSTRACT

Central nervous system (CNS) sustained injuries in mammals often result in severe and irreversible damage, with CNS regeneration being limited due to the restricted regenerative potential of neurons. Yet, CNS regeneration is possible in embryos, and its regenerative potential stops very early after birth. *Monodelphis domestica*, the grey short-tailed opossum, is a pouch-less marsupial born at a very immature state, equivalent to embryonal day (E)13 in rats or E12.5 in mice. The initial development of their cortical plate occurs at postnatal day (P)3-5 and gliogenesis begins around P18. Moreover, these opossums have an extraordinary ability to fully regenerate their spinal cord up to two weeks after birth, with their regenerative ability declining with the rise of non-neuronal cells. Therefore, they are a great animal model to study CNS development and regeneration potential *in vitro*. Primary cell cultures derived from their cortices were obtained and examined at different developmental ages, P6 and P17. The cellular composition of primary cortical cell cultures was best characterized in P6 opossums with immunofluorescence microscopy. TUJ1+ neuronal population rose from 60% at days *in vitro* (DIV)1 to its peak 84% of neurons at DIV5, and further declined to 44% at DIV13. Astrocytes showed maturation from DIV5 to DIV13, accounting for 28% to 32% of GFAP+ cells, respectively. Neuronal and non-neuronal cells' regenerative potential within the CNS was examined with an induced injury in both P6 and P17 cortical cultures, performed with a scratch assay. P6 cultures did show a better regenerative performance, as neurons regenerated and grew their axons across the cut site, forming growth cones (GCs) which differed in size with age. Astrocytes polarized their processes along the cut site or migrated to the cut, resembling glial scar formation. Opossum primary cortical cultures provide, therefore, an additional and novel source of mammalian cells for *in vitro* investigations.

**Keywords:** *M. domestica*, CNS regeneration, development, primary cortical cell cultures, injury

## SAŽETAK

Ozljede središnjeg živčanog sustava (SŽS) kod sisavaca često rezultiraju teškim i nepovratnim oštećenjima, pri čemu je regeneracija SŽS-a ograničena zbog ograničenog regenerativnog potencijala neurona. Ipak, regeneracija SŽS-a moguća je u embrijima, a regenerativni potencijal prestaje ubrzo nakon rođenja. *Monodelphis domestica*, sivi kratkorepi oposum, je tobolčar bez pravog tobolca čiji su mladunci rođeni vrlo nerazvijeni, ekvivalentno embrionalnom danu (E)13 kod štakora ili E12.5 kod miševa. Početni razvoj njihove kortikalne ploče događa se postnatalnog dana (P)3-5, dok gliogeneza počinje pri P18. Nadalje, oposumi imaju izvanrednu sposobnost potpune regeneracije svoje leđne moždine i do dva tjedna nakon rođenja, pri čemu njihova regenerativna sposobnost opada s porastom ne-neuronskih stanica. Stoga, oposumi su izvrstan životinjski model za proučavanje razvoja SŽS-a i regenerativnog potencijala *in vitro*. Primarne stanične kulture pripremljene iz korteksa ispitane su u različitim razvojnim dobima, P6 i P17. Stanični sastav primarnih kortikalnih staničnih kultura najbolje je karakteriziran kod P6 oposuma s imunofluorescentnom mikroskopijom. TUJ1+ neuronska populacija porasla je sa 60% pri *in vitro* danu (DIV)1 do vrhunca - 84% neurona pri DIV5, s padom na 44% pri DIV13. Astrociti sazrijevaju sa razvojem, od DIV5 do DIV13 njihova je populacija porasla sa 28% na 32% GFAP+ stanica. Regenerativni potencijal neuronskih i ne-neuronskih stanica unutar središnjeg živčanog sustava ispitan je s induciranom ozljedom u kortikalnim kulturama P6 i P17, simuliranom sa testom reza. P6 kulture su pokazale bolji regenerativni potencijal, pri čemu su neuroni regenerirali i izrasli aksone kroz mjesto reza, stvarajući konuse rasta različitih veličina ovisno o dobi. Astrociti su polarizirali, pri čemu su se njihovi izdanci izdužili okomito na mjesto reza ili su migrirali na mjesto, predstavljajući stvaranje glijalnog ožiljka. Primarne kortikalne kulture dobivene iz oposuma je nov izvor stanica sisavaca koji doprinosi *in vitro* istraživanjima.

**Ključne riječi:** *M. domestica*, regeneracija i razvoj SŽS-a, primarne kortikalne stanične kulture, ozljeda



## CONTENTS

1	INTRODUCTION.....	1
1.1	The composition of central nervous system.....	1
1.1.1	Neurons and neuronal development.....	2
1.1.2	Glial cells and gliogenesis .....	6
1.1.3	Adult neurogenesis .....	8
1.2	Traumatic injury and limitations of regeneration in CNS .....	8
1.2.1	Dual role of inflammation .....	10
1.2.2	Axonal regeneration.....	11
1.2.3	The formation of a glial scar.....	12
1.3	<i>Monodelphis domestica</i> as a studying model for neuronal regeneration.....	13
2	AIM OF THE THESIS .....	15
3	MATERIALS AND METHODS.....	17
3.1	Animals.....	17
3.2	Primary neuronal cell cultures .....	17
3.2.1	Preparation of mounting coverslips .....	17
3.2.2	Dissociation and plating of primary neuronal cultures.....	18
3.2.3	Scratch assay for neuronal regeneration.....	20
3.3	Immunofluorescence.....	21
3.3.1	Immunocytochemistry (ICC) .....	21
3.3.2	EdU staining .....	21
3.3.3	Antibody solutions .....	22
3.4	Fluorescence microscopy .....	25
3.5	Data analysis .....	26
4	RESULTS .....	28

4.1	Primary neuronal cell cultures from <i>Monodelphis domestica</i> cortexes.....	28
4.2	Cellular identification and culture maturation within different age groups .....	28
4.2.1	Markers for cellular identification .....	28
4.2.2	Neurogenesis and neuronal identification using ICC .....	28
4.2.3	Identification of glial cells .....	34
4.3	Cellular behaviour and the regenerative capacity of primary cell cultures upon an induced injury <i>in vitro</i> .....	38
4.3.1	Cellular fate upon injury: proliferation and death .....	41
4.3.2	Regeneration and glial scar formation in different <i>M. domestica</i> developmental ages .....	45
4.3.3	Growth cones versus retraction bulbs (following <i>in vitro</i> injury)	46
5	DISCUSSION.....	48
6	CONCLUSIONS .....	55
7	REFERENCES.....	56

# **1 INTRODUCTION**

## **1.1 The composition of central nervous system**

The nervous system has the extraordinary capability to process and respond to various physiological and pathological stimuli. The central nervous system (CNS), along with the peripheral nervous system (PNS), makes a part of this complex and highly specialized structure. The CNS contributes as an information-processing system, conducting regulation of all physiological functions within an organism, independently of other systems within the body <sup>1</sup>.

The CNS consists of spinal cord and brain, with further division of brain into cerebellum, thalamus and two cerebral hemispheres <sup>2</sup>. Because of their locations within the skull and vertebral column, both brain and spinal cord are the most protected structures in the body <sup>3</sup>. At the histological level, the main cell types that comprise the CNS are neurons and glial cells. Neurons are considered to be the main functioning unit in the CNS. They generate and transmit information in the form of action potential, expressing their function within the entire body due to the connections between CNS and PNS neurons. This allows the neurons to transmit information in a quick manner over longer distances. Neurons do that by processing received signals, resulting in an integration of these signals and transmission of an appropriate response to a neighbouring neuron or to an effector, such as a muscle or a secretory cell. The signals can be received either from the environment, in the form of chemicals released at the junctions from other neurons or as electrical signals admitted through low-resistance gap junctions between neighbouring neurons. The supporting cells, known as glia, play a vital role in the maintenance of the nervous system homeostasis, allowing proper neuronal function <sup>4,5</sup>. The estimated ratio between glial cells and neurons in the human brain, obtained with a counting method – isotropic fractionator, is close to 1:1, contrary to the traditional view that the two main cells coexist in a 10:1 relation in favour of glial cells <sup>6</sup>.

### 1.1.1 Neurons and neuronal development

With only a few exceptions, the vast majority of neurons are comprised of three parts: a cell body, also known as soma, from which further extend one axon and many short, branched, filamentous processes called dendrites (Figure 1). Dendrites are responsible for receiving most of the inputs from other cells and propagating signals, while axons extend from the soma to the adjacent cell, making a contact. Axons generate electrical signals, or action potentials, at their beginning – the axon hillock. The signals are further propagated through the axon until they reach the branched ending, where the signals are further transmitted through synapses to either another neuron or an effector. Two types of synapses exist: electrical and chemical. Electrical synapses connect two cells with a gap junction and their channels allow the passage of small molecules, such as ions. They are bidirectional. Chemical synapses are connected through a synaptic cleft, a gap in which neurotransmitters are released to target receptors of the receiving cell. The axonal length can range from a few millimetres up to a meter, such as in motor neurons that supply muscles <sup>1</sup>.

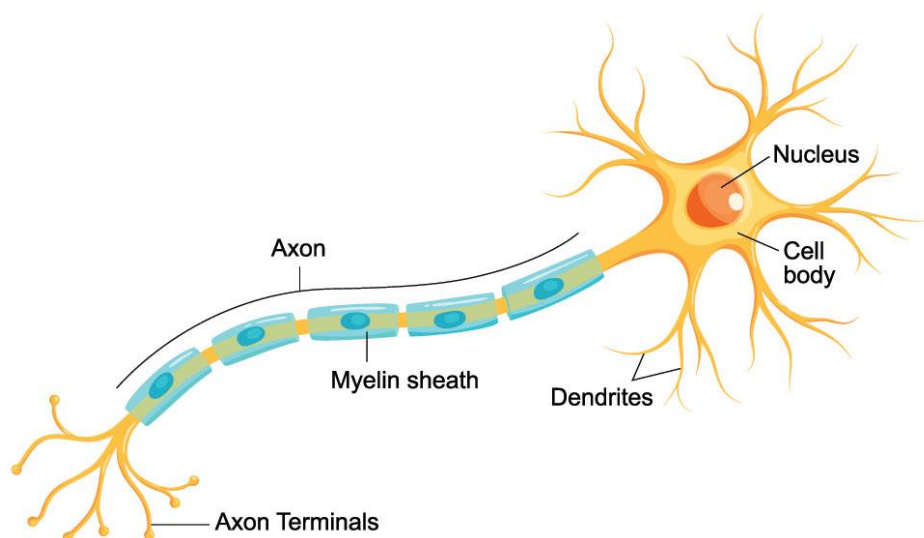


**Figure 1** Schematic overview of a neuron, showing the cell body from which emerge dendrites, short and filamentous processes and one extended axon with belonging terminals that form synaptic ends. Source: Vitalii Dumma, Getty Images Plus.

Essentially, development of all nervous systems takes four crucial stages: the proliferation of progenitors, the differentiation into neurons or glia, the growth of axons and dendrites, and finally, formation of electrical and chemical synapses. Moreover, organisms such as mammals have a more complex organisation of nervous system and have an additional migration step, in which newly specified neurons migrate before they differentiate to form synapses <sup>7</sup>. During the maturation of a gastrula, three germinal layers are developed: endoderm which precedes the development of primordial viscera (the intestines), mesoderm preceding the development of primordial bones and muscles, and ectoderm, preceding the primordial nervous system and skin. Over time, ectodermal cells form a flat sheet, also known as the neural plate, which develops into a cylinder of cells known as the neural tube. The neural tube is comprised of multipotent neural progenitor cells (NPCs), previously derived from embryonic stem cells (ESCs), which can divide symmetrically, allowing them to build up the precursor cell pool in a self-renewing fashion during the development of the neural plate. They also bear the potential to divide asymmetrically to generate neural and glial cell precursors (Figure 2), such as radial glia. However, NPCs do not generate non-neural cells, such as microglia that belong to the immune system cells of the brain <sup>8-10</sup>.

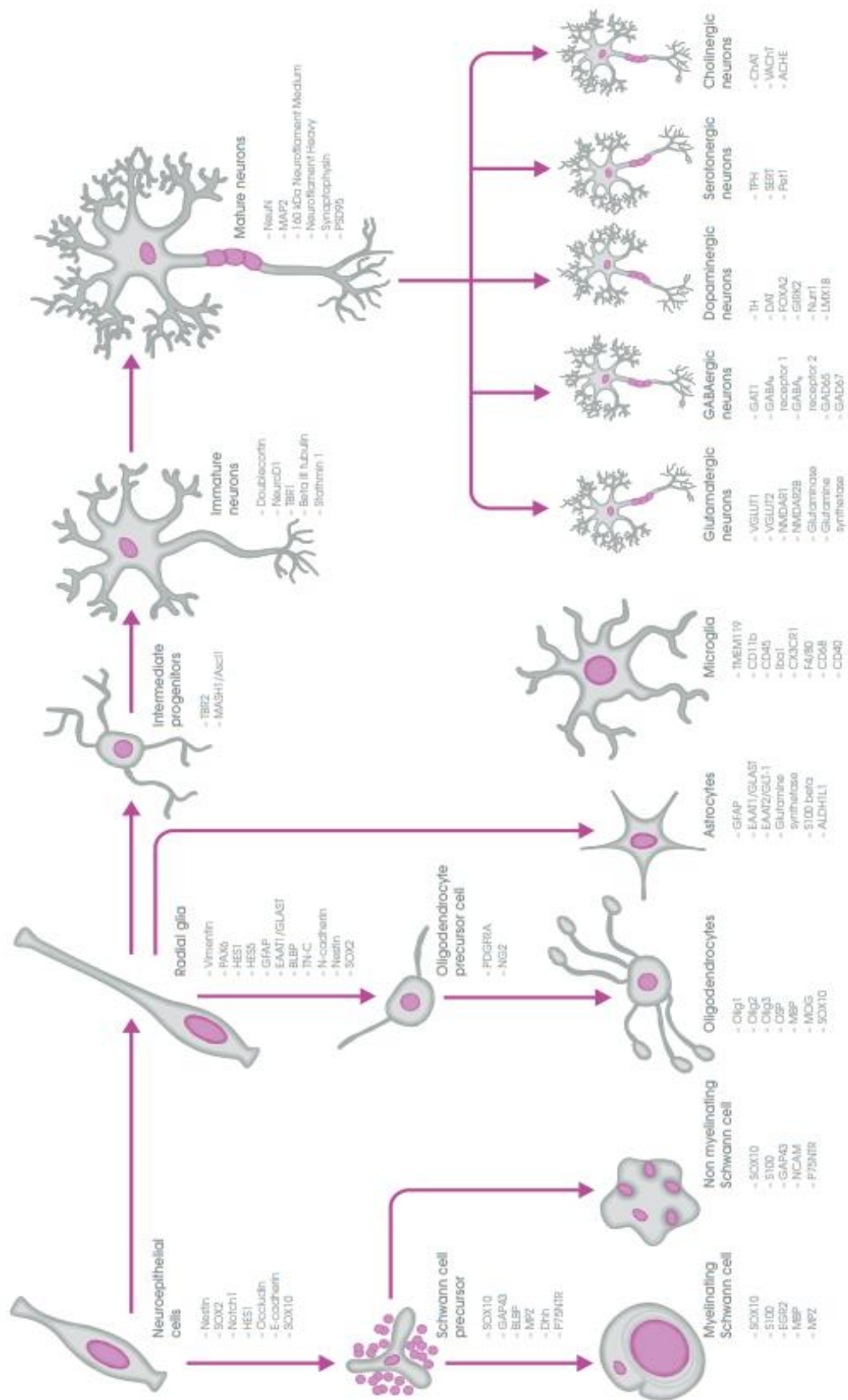


**Figure 2** Schematic representation of the NPC developmental potential to neural and glial cells in the CNS. Source: [abcam.com/neuralmarkers](http://abcam.com/neuralmarkers).

Radial glia cells (RGCs) have several important roles in the genesis and placement of neurons during their development in the brain. RGCs are derived from NPCs and retain their ability to further divide and play a precursor role that gives origin to all major classes of neural and glial progenitors (Figure 2). RGCs are characterized by their bipolar shape, oval nuclei, and two processes: one short, apical process terminating at the ventricular surface, and one longer, basal process terminating at the cerebral surface. They are abundantly localized in the ventricular zone (VZ) during brain development, where they are organized in a radial orientation and express glial markers, originating their name <sup>11</sup>.

Generally, neurogenesis precedes gliogenesis in the developing CNS, a process that can be achieved through two available mechanisms: RGCs initially give rise to neurons followed by development of glia, meaning that RGCs are in this case either bi- or multipotent. Other mechanism subsets distinct subtypes of RGC, where one subtype specifically generates neurons, while the other primarily gives rise to radial glia which later develop into astrocytes <sup>12</sup>.

RGCs not only contribute to neurogenesis, but also provide guidance for neuronal migration from their proliferative VZ and subventricular zone (SVZ) to the distant cortical plate through a radial pathway constructed of single or often more RGC fibres. These fibres are attached to the ventricular surface, allowing newly generated neurons to migrate along the fibre of the mother cell. The daughter cells are further guided by the radial fibres of their mother's cell to their destination in the developing cortical plate<sup>11</sup>. This migration is also known as radial migration, allowing the expansion of thickness of the neural tube. Neurons can also migrate in a tangential fashion, parallel to the ventricular surface and orthogonal to the radial glia palisade. During migration, neurons are polarized in the movement direction: leading processes of migrating axons are tipped by dynamic membrane extensions called lamellipodia and filopodia, structures that form neuronal growth cones (GCs), contributing to the

sensing of the microenvironment and guidance of the neurons. Proper neuronal migration is necessary for further synapse formation and assembly of the neural circuitry <sup>13</sup>.

Neural circuits precede other diverse functional capacities of the brain as the primary supracellular mediator of these functions. It is a network of clustered neurons that receive electrochemical signals, processing them to further transmit a signal to other circuits for additional modification. When neurons successfully complete their migration, they form synapses by extending their axons and dendrites to neighbouring cells. The migrated neurons and synaptic connections that rise early in development pose as transient stages, or scaffolds, for future stable connections, moulding the circuitry until appropriate postsynaptic neurons are in their place<sup>14</sup>.

### **1.1.2 Glial cells and gliogenesis**

In the 19<sup>th</sup> century, as they were first identified, glial cells were considered solely to pose as “nerve glue”. This assumption was abolished through numerous years of research, characterizing their actual functions within the CNS as homeostatic: maintaining cells of the brain. Glial cells can be divided into four major subgroups: microglia, astrocytes, oligodendrocytes, and NG2-glia, oligodendrocyte progenitors <sup>5,15</sup>.

Microglia are the immunocompetent cells of the nervous system, usually rendered as the macrophages of the nervous system. They are characterized as scavenger cells when the CNS is immunocompromised or damaged, such as in the event of infection, inflammation, neurodegeneration, or ischemia <sup>16</sup>. Microglia have a different origin in comparison to other CNS cells: they originate from yolk sac-primitive macrophages, persisting in the CNS through its development into adult age. Microglial colonization in the early embryonic brain in different vertebrate species implies their importance for early brain development <sup>17</sup>.

The glial cells that are one of the most abundant within adult brain are astrocytes. Astrocytes are closely associated with synapses throughout



the development of the brain, contributing to the synapse formation through contact-mediated signals and secreted signals. They also contribute to the synaptic strength, stabilizing their structure, and regulating the elimination of preceding pre-established synapses. Other supporting functions that allow optimal brain and neuronal function include uptake of the excitatory amino acid transmitter glutamate, preventing glutamate excitotoxicity. They also produce lactate through stimulation of neuronal activity, which is then fed to neurons and further processed to enter the Krebs cycle for ATP production. Moreover, astrocytes contribute to the maintenance of water and ion homeostasis, as well as to the blood brain barrier (BBB) maintenance and formation, of which astrocytes are a component. Recent discoveries confirm their role in higher brain functions including sleep homeostasis, memory and learning <sup>5,15,18-20</sup>.

Mature oligodendrocytes are cells that produce myelin, electrically insulating the axons with their own cell membrane in a spiral shape. This allows for a rapid propagation of electric potential and gives a trophic support to axons <sup>21</sup>.

NG2-glia, oligodendrocyte progenitors, keep the lineage by producing mature oligodendrocytes throughout the lifetime with the ability to myelinate axons, maintaining cell number homeostasis under physiological conditions <sup>15</sup>.

As mentioned previously, neurogenesis precedes gliogenesis, but the two processes still overlap in several brain regions. In correlation with the end of neurogenesis, neurogenic RGCs diminish and finally disappear, while the remainder of RGCs develop into astrocytes during gliogenesis. This also results in the lack of RGCs in the adult mammalian brain, limiting the genesis potential of neuronal cells <sup>12</sup>.

### **1.1.3 Adult neurogenesis**

Most regions in the mammalian brain develop their full complement of neurons in prenatal development, with each neuronal population generated at a specific time window in brain development <sup>22</sup>. Active adult neurogenesis constitutively occurs in specific regions of the adult CNS, such as the olfactory bulb, dentate gyrus of the hippocampus, and subventricular zone of lateral ventricles, and is dependent on the microenvironment of these regions. In non-neurogenic regions, the adult mammalian brain contains a certain number of multipotent neural precursors: local parenchymal precursor cells might be activated by environmental events, such as a pathological event or molecular and genetic interventions. Moreover, precursor cells from neurogenic regions might migrate to parenchyma in response to the said stimuli. Adult CNS “stem cells” feature self-renewal, theoretically having unlimited ability to divide symmetrically<sup>23</sup>. They are proliferative, and they can be multipotent for different CNS neuroectodermal cell lineages, as confirmed upon their isolation and successful propagation *in vitro* <sup>24</sup>. Multipotent cells have a limited self-renewal cycle, allowing them to only differentiate into at least two different cell lineages. When undifferentiated, NPCs of the adult brain are characterized as highly mobile cells, resistant to certain injuries, including hypoxia, proliferative, and able to produce both neurons and glia. When these cells differentiate into new cells, their integration depends on complex variables and progressive events within their environment. Moreover, NPCs in the adult mammalian brain are heterogenous, expanding their abilities <sup>23</sup>. Adult neurogenesis and the presence of adult NSCs provide great hope for future therapies, treating trauma and injuries within the CNS.

### **1.2 Traumatic injury and limitations of regeneration in the CNS**

CNS injuries, caused by both intrinsic and extrinsic factors, often result in irreversible damage because axons fail to regenerate. These injuries are characterized by two stages: primary and secondary injury.

Primary injury is defined as the initial mechanical damage in CNS trauma. Primary injuries to the spinal cord by direct forces cause shearing, compression, contusion, or transection, while traumatic brain injuries are caused by axonal stretch, haemorrhage, and cerebral contusion<sup>4</sup>.

Secondary injury (Figure 3) is initiated by a cascade of molecular and cellular events, further transitioning the injury into acute, subacute, and chronic stages. The acute phase is characterized by direct neuronal and glial cell injury and death within the first 48 hours of the trauma, causing disruption in cellular ion homeostasis and neuronal circuitry. Moreover, the environment becomes more hostile due to the upregulation of chemokines, cytokines, and reactive oxygen species (ROS). The subacute phase is characterized by events up to two weeks after injury. In the two-week span, the injury environment begins to mature, releasing inhibitory neurite growth factors, which limit axonal sprouting and inflammatory changes occur. This phase is also characterized by reactive gliosis within the CNS, causing a glial scar by proliferating glial cells near the injury site, limiting functional plasticity and regeneration. Finally, during the chronic stage, 6 months after the injury, remodelling acts in forming new circuitry and axonal sprouting <sup>4</sup>.

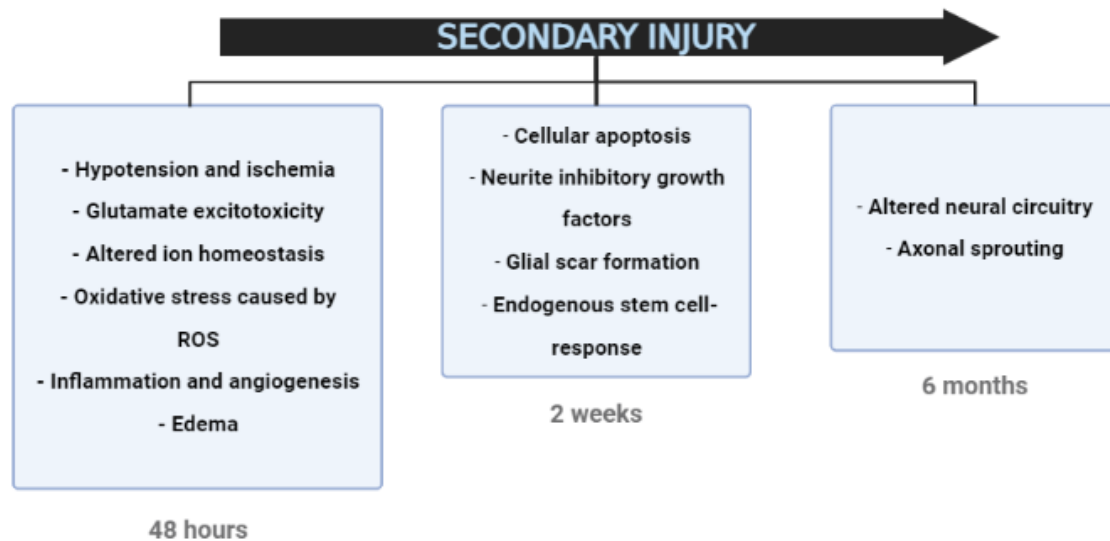


**Figure 3** Schematic overview of mechanisms and events that characterize secondary injury. Created with BioRender.com.

### 1.2.1 Dual role of inflammation

The immune system normally reacts to sustained injuries within the organism, minimising degeneration and reacting to the debris within the CNS. Within minutes following the injury, proinflammatory cytokines are released on site, promoting acute effects with defective consequences, such as blood-brain barrier (BBB) dysfunction and neuronal death. The same cytokines are beneficial at later stages of an injury by inducing synthesis of anti-inflammatory cytokines, secretion of neurotrophic factors, and proliferation of precursor cells for oligodendrocytes, helping in remyelination. Similarly, complement proteins are involved in BBB dysfunction, but later contribute to the elevated production of growth factors <sup>25</sup>.

On a cellular level, microglia are the first to react to the sustained injury by proliferating, activating, and migrating. A dysfunctional BBB with increased permeability allows infiltration of immune cells to injury sites, which is guided by cytokines, complement proteins and chemokines. Immune cells release ROS, harming the environment, but aid debris and

damaged cell removal. These processes of inflammation and their duality throughout different injury phases pose as a challenging target for treatment of injuries sustained within the CNS <sup>25</sup>.

### **1.2.2 Axonal regeneration**

Downstream signalling events in secondary injury are not the only factors inhibiting axonal regrowth. Another obstacle in their regeneration is the decline in intrinsic capacity of the axon growth that is age-dependent, meaning that mature neurons have a receding potential for successful axonal regeneration. Moreover, gene expression regulating the regeneration must be coordinated with cytoskeletal dynamics to ensure efficient reassembly of structural components and distribution of signalling molecules. This event results in the sprouting of a new growth cone (GC), causing forward movement, ensuring axonal growth. The GC is a sensory motile structure on a tip of a growing neurite (Figure 4A). It is enriched with microtubules within the central domain, with actin filaments enriching the peripheral domain. While actin filaments play a central role in pathfinding decisions and guiding microtubules in response to environmental signals, microtubules pose as building blocks of an axon, allowing axon extension through the formation of lamellipodia and filopodia. They're vital for axon growth and guidance by exploring intracellular space, interacting with signalling molecules, and reorganization in response to the signals <sup>26,27</sup>.

Destabilization of GC's organized microtubule network results in the formation of a bulb-like structure, called a retraction bulb (RB). The RB consists of depolymerized, disorganized microtubules with no separate domains of F-actin (Figure 4B). These dysregulated dynamics contribute to the inability of regeneration in adult neurons in the CNS, and engage growth-inhibitory signal cascades, resulting in activation of scar-forming cells among astrocytes and fibroblasts within the injury <sup>26,27</sup>.

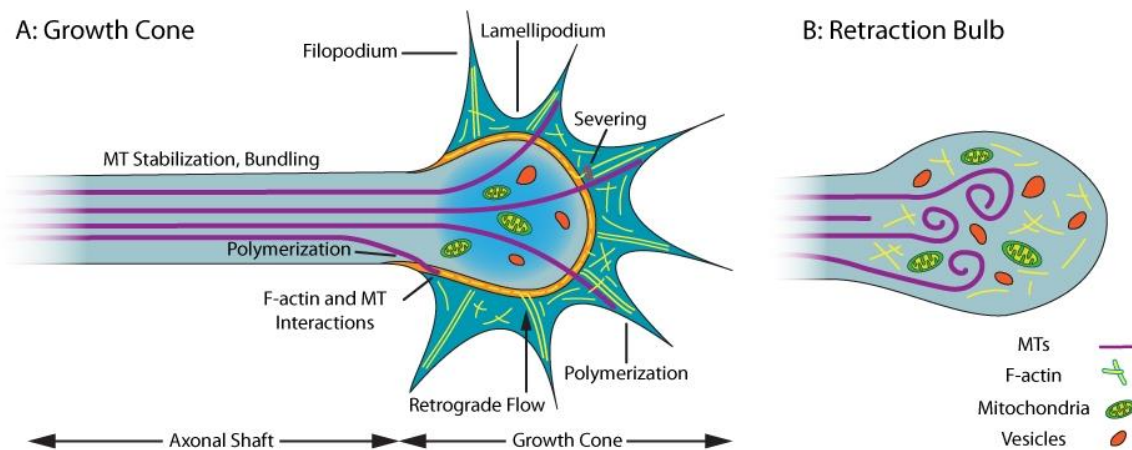


**Figure 4** Different morphologies of a growth cone (GC) and a retraction bulb (RB). The dynamics of F-actin and microtubules allows the extension of lamellipodia and filopodia necessary for axon elongation. Retraction bulb is a result of faulty microtubule assembly, resulting in their depolymerization and prevention of axon regeneration. Source: [cytoskeleton.com/axon-regeneration-and-the-cytoskeleton](https://cytoskeleton.com/axon-regeneration-and-the-cytoskeleton)

### 1.2.3 The formation of a glial scar

Activated glial cells, including astrocytes and microglia, migrate to the injury site and form an interpenetrating network known as the reactive glial scar. The initial, beneficial roles include aforementioned isolation of the injury site, defence against cytotoxic molecules, and BBB repair. When these cells persist at the injury site, inhibitory factors, which limit axonal regeneration, are produced. As a regenerative response, new GCs can form and sprout short distances from severed axons within the injury site, before receding due to the inhibitory chemical environment <sup>25</sup>.

Upon 2-3 days after an insult, transient upregulation of glial fibrillary acidic protein (GFAP) is evoked, along with withheld proliferation of reactive astrocytes. Upregulated GFAP causes cell body hypertrophy associated with interpenetrative extension of distant processes. In this way, astrocytes in the vicinity of a lesion form a border, orient, and extend their long processes towards the injury site, forming palisades, 1 week after the initial lesion. The more distant the astrocytes are to the injury site, the less they resemble the astrogliosis hallmarks,

aforementioned hypertrophy and upregulated GFAP levels, which seem to decrease <sup>28</sup>. A close schematic representation can be seen in Figure 5. Glial scarring is essential for the initial tissue protection after an injury, and as reactive astrocytes can be, they protect against the further spread of inflammation and cell death. Palisading astrocytes near the lesion sites stay reactive permanently, while distant astrocytes return to their normal state <sup>29</sup>.

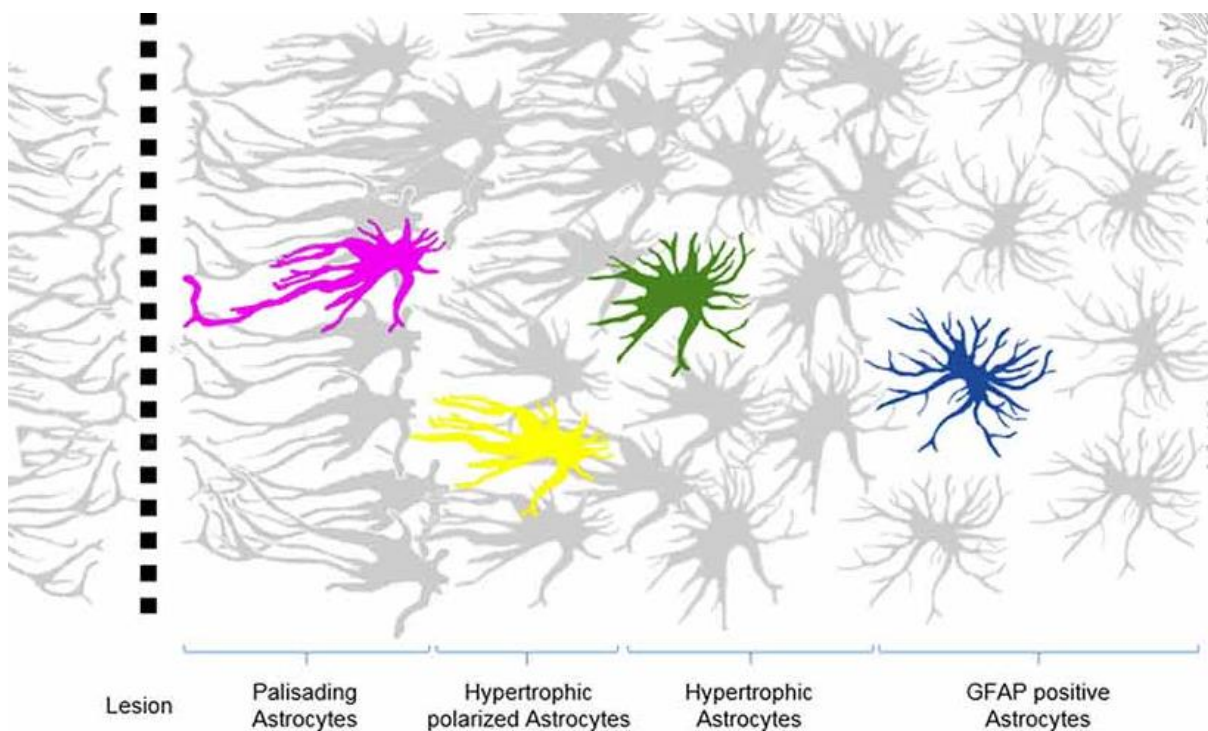


**Figure 5** Schematic representation of a lesion within the CNS and astrocytic mobilisation. Astrocytes in the vicinity of a lesion tend to be more hypertrophic and have elevated GFAP levels. These hallmarks help them in the formation of "palisades" by extension of their processes, orienting them to form a border. The further astrocytes are from the lesion site, the more they seem to have decreased astrogliosis hallmarks. Source: Schiweck et al. (2018).

### 1.3 *Monodelphis domestica* as a model for studying neuronal regeneration

*Monodelphis domestica*, the South American grey short-tailed opossum, is a nocturnal rodent-like, pouch-less marsupial native to Brazil <sup>30</sup>. In suitable vivarium conditions, they breed all year long with an oestrous cycle of approximately 28 days, with up to 11 pups in a litter. They are

born at a very immature state after a gestational period of 14 days. Developmentally, in postnatal days (P) 3-5 they are equivalent to a 15.5-18.5 embryonal day (E) rat or E14-16 mice, while P16-18 pups correspond to P1-2 rats and mice <sup>31</sup>. Although immature, neonates have developed suckling, breathing, and climbing from the birth site to the teat. This development is also apparent physically, as their frontal systems are developed before their hinder parts, giving an insight into the rostro-caudal gradient of development. The cortical plate starts appearing at around postnatal day 3 to 5, allowing the study of its development in postnatal pups, with neocortex being apparently mature after 45 to 60 days, around the weaning period of pups <sup>32</sup>.

There are several advantages of using the isolated CNS of *M. domestica* pups as a model system. Neonate pups are easily accessible and collected given that their mothers lack pouches, which prevents the need for intrauterine surgery procedures on the mother. At early postnatal ages, pups are not longer than 1.5 cm, allowing the entire isolated CNS survival *in vitro* <sup>33</sup> and suitability for microsurgical manipulations of CNS structures such as cortexes and spinal cord *ex utero* <sup>34</sup>. Moreover, following injury, they are able to fully regenerate their spinal cord up for to two weeks after birth<sup>33</sup>. The ability to regenerate abruptly stops around P12 in the cervical part of the spinal cord, and at P17 in lumbar parts of the spinal cord. In concordance, gliogenesis starts generating astrocytes at P18, with oligodendrocytes being produced last around P40<sup>34</sup>. Primary dissociated cortical neuronal cultures derived from opossums have only recently been established; P3-P5 opossum cortexes yield almost pure neuronal cultures, while P16-P18 neuronal cultures have a lower yield of neuronal population as a result of the rise of non-neuronal cells, including astrocytes and microglia <sup>35</sup>.



## 2 AIM OF THE THESIS

*M. domestica* are animals with great potential as a model system for studying mammalian CNS development and the impact of injuries. This species breeds throughout the year, and therefore it is easy to maintain their colony and obtain the pups. Newborn pups are characterized by their largely undeveloped CNS, whose cortices and spinal cords can be feasibly extracted and cultivated. Moreover, neuronal regeneration in *M. domestica* is age-dependent, with its regenerative potential stopping between postnatal days 9 and 12. Since these are recently established cultures <sup>35</sup>, there is a lot of additional work required to fully characterize their properties, as it has been done with primary cultures derived from rats or mice. Therefore, expression of additional markers has to be validated and compared between different postnatal age of opossums (P6 vs P16) as well in different days of culture (DIV):

The first aim of this thesis was to further investigate the properties of primary cortical neuronal cell cultures derived from neonatal opossums, *M. domestica*. Since these are recently-established cultures <sup>35</sup>, there is a lot of additional work required to fully characterize their properties, as it has been done with primary cultures derived from rats or mice. Therefore, expression of additional markers has to be tested and compared between different postnatal age of opossums (P6 vs P16) as well in different days of culture (DIV1, DIV5, DIV13 and DIV20). This will allow the proper characterization of cells within the culture, which is the second aim of the thesis. This involved obtaining cortices from different neonatal ages, postnatal day 6 and 17 (P6 and P17). The cultures were prepared following the establishment protocol published by Petrović et al. <sup>35</sup>.

The third aim of the thesis is to investigate cell response to the *in vitro* injury using different markers for neuronal and glial cells.  $\beta$ -tubulin III and vimentin were used for characterization in the majority of samples, while GFAP, GAP43, and S100 $\beta$  were used for further identification of the cells. In this way, it is possible to detect the difference between cell populations

given the age difference, since it's been established that neurogenesis precedes gliogenesis. P6, therefore, offers a way to study neuron-intrinsic properties, while with P17 cultures we can examine the crosstalk between different cell types and the more complex response after injury.

After successful establishment of cultures and cell identification, the last aim was to detect cell behaviour in the region of the cut, whether neurons undergo regeneration, i.e., if axon tips form growth cones (GCs) or retraction bulbs (RBs), if the regeneration is defective, and whether activation and mobilisation of glial cells with glial scar formation occurs *in vitro*. Furthermore, the goal was to see and compare growth cone size 24 hours after the cut, and whether they change with age of cultures. In addition to GCs, the goal was to characterize RBs as well.

### **3 MATERIALS AND METHODS**

#### **3.1 Animals**

South American grey, short-tailed opossums, *Monodelphis domestica* were used for this research. Both sexes of the pups were used, at two different postnatal (P) ages: P6 and P17. The colony is bred at the vivarium facility of the University of Trieste, following the guidelines of the Italian Animal Welfare Act. The use of opossums was approved by the Local Veterinary Service, the Ethics Committee board, and the National Ministry of Health (According to the Permit Number: 1FF80.N.9Q3), following the European Union guidelines for animal care (d.1.116/92; 86/609/C.E.). The opossums were maintained in standard laboratory cages in a controlled environment (27°C-28°C temperature; 50%-60% humidity), with a 12/12 light and dark cycle and *ad libitum* access to food and water. The experiments were performed in accordance with the European Directive 2010/63/EU for animal experiments. All experiments followed the "3R" principle: reduce, replace, and refine, minimizing the number of animals used as well as their suffering.

#### **3.2 Primary neuronal cell cultures**

The dissociation protocol followed the already established protocol prepared and optimized by Petrović et al.<sup>35</sup>. Instruments and all working surfaces that were used in this protocol were precleaned and disinfected with 70% ethanol (Gram-mol, Zagreb, Croatia) and 1% Incidin (Ecolab, Zagreb, Croatia). All the solutions that will be further mentioned needed to be sterilized and filtrated through a 0.22 µm syringe filter (Carl Roth, Karlsruhe, Germany).

##### **3.2.1 Preparation of mounting coverslips**

12 mm diameter coverslips (Thermo Fisher Scientific, Waltham MA, USA) were stored in 25 mL Falcon tubes containing 1 M hydrochloric acid (Ru-Ve, Sveta Nedjelja, Croatia) and shaken 4 times every 30 minutes to ensure equal coating and bathed overnight at room temperature (RT; 20°C-22°C). The bath was followed by a thorough wash, 5 times per

batch with autoclaved water and a final wash with 96% ethanol at RT for an hour. Coverslips were then spread in a glass Petri dish and dry sterilized in the oven at 150°C for 90 minutes. This allows the coverslips to be used for the next two months. After sterilization, the coverslips were placed in all wells of a 24-well tissue culture plate (Sarstedt, Nümbrecht, Germany) and coated with 100 µL of 50 µg/mL poly-L-ornithine (PO, Sigma-Aldrich, Saint Louis, MO, USA), overnight at 32 °C. The next day, PO was removed, and the coverslips were further coated with 2 µL/mL laminin (Sigma-Aldrich), diluted in a 1:500 ratio for cortexes.

### **3.2.2 Dissociation and plating of primary neuronal cultures**

To obtain enough primary neurons for a full 24-well plate, two cortical hemispheres of two opossums were dissected per postnatal age (P6 and P17). Opossums were decapitated with scissors. For this experiment, only heads were further dissected in a pre-cooled oxygenated (95% O<sub>2</sub>/5% CO<sub>2</sub>; 15 minutes) Krebs dissection solution (113 mM NaCl, 4.5 KCl, 1 mM MgCl<sub>2</sub> x 6H<sub>2</sub>O, 25 mM NaHCO<sub>3</sub>, 1mM NaH<sub>2</sub>PO<sub>4</sub>, 2 mM CaCl<sub>2</sub> x 2H<sub>2</sub>O, 11 mM glucose and 0.5 % w/v Penicillin/Streptomycin/Amphotericin B, pH 7.4; Sigma-Aldrich). The hemispheres were isolated by removing olfactory bulbs, meninges, and remaining subcortical structures. The dissected tissue was severed into small pieces, washed three times with cold sterile phosphate-buffered saline (PBS) solution (137 mM NaCl, 2.7 mM KCl, 10 mM Na<sub>2</sub>HPO<sub>4</sub>, 2 mM KH<sub>2</sub>PO<sub>4</sub>; Sigma-Aldrich). Cortices were then digested enzymatically with prewarmed trypsin (32°C) in EDTA (Santa Cruz Biotechnology, SCBT, Dallas, TX, USA). Cortices were digested in 0.5% w/v trypsin for 10 minutes and 2.5% w/v trypsin for 15 minutes for P6 and P17 pups, respectively, incubating on a thermoblock set at 32.5°C. Following the incubation, a triple wash in PBS was performed followed by trituration of the tissue in a trituration solution comprised of 10 mg/mL DNase I (Sigma-Aldrich), 1mg/mL trypsin inhibitor (SCBT), and 1% w/v bovine serum albumin (BSA; Pan-Biotech, Aidenbach, Germany) in Hank's Balanced Salt solution (HBSS) without Ca<sup>2+</sup> and Mg<sup>2+</sup> ions (Pan-Biotech),

isolating cells from the tissue. The trituration was performed by mechanical pipetting, using a 500  $\mu$ L filter-containing tip at least 15 to 30 times. Larger tissual pieces were left to sediment on the bottom, while the cell supernatant was collected with repeated trituration two and three times, for P6 and P17 pups, respectively. It was necessary to avoid foaming during the trituration process as it can damage and kill the cells. The supernatant with isolated cells was layered on top of 5% w/v BSA solution in HBSS to remove cell debris. Cells were centrifuged at 1000 rpm for 6 minutes at 4°C, followed by supernatant removal. Cells were then resuspended in plating medium consisting of Dulbecco's minimum essential medium (DMEM) with stable glutamine, supplemented with 10% w/v foetal bovine serum (FBS) and 1% w/v Penicillin/Streptomycin (all from Pan-Biotech). An additional 1 mL of the plating medium was added to the suspension, and it was transferred into the 35 mm Petri dish (Sarstedt) through a 70  $\mu$ m cell strainer (Corning Inc., Corning, NY, USA) for pre-plating. The cell suspension was incubated at 32°C for 5 minutes and collected, then diluted in plating medium in 15 mL tubes (Carl Roth) to the  $5 \times 10^4$  density (500  $\mu$ L) of cells per well for a 24-well plate. The diluted cell suspension was only placed in inner wells, while the wells on the edge of the plate were filled with 500  $\mu$ L H<sub>2</sub>O. The cells were then incubated overnight, followed by replacing 2/3 of plating medium with fresh, prewarmed neuronal medium containing Neurobasal medium, supplemented with B27 (all from Thermo Fisher Scientific) 24 hours after plating. Media was changed once per week, each time replacing half of the medium with fresh, prewarmed neuronal medium. Primary cortical cultures were further maintained in an incubator at 32 °C with 5% CO<sub>2</sub> and 95% relative humidity.

The dissociation protocol is schematically represented in Figure 6 for easier understanding.

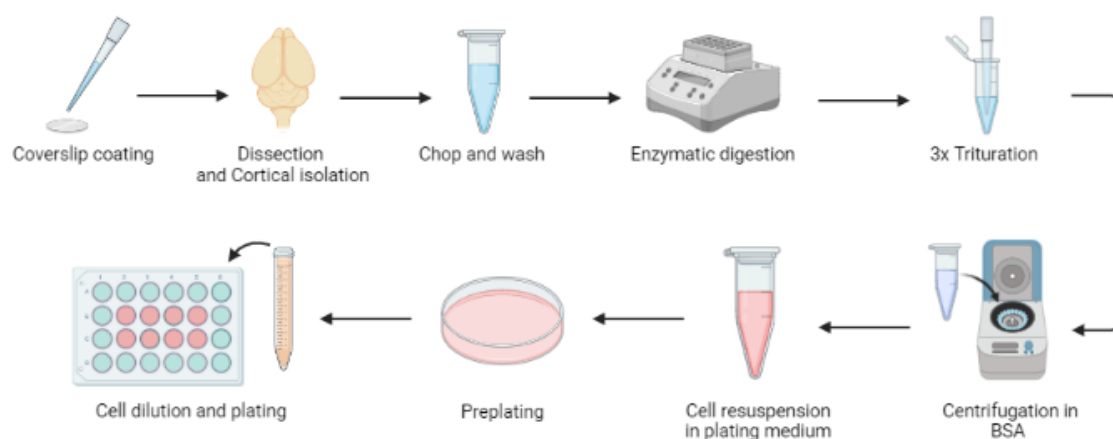


**Figure 6** Schematic representation showing the process of obtaining primary cortical neuronal culture from the cortices of *M. domestica*. Created with BioRender.com.

### 3.2.3 Scratch assay for neuronal regeneration

After plating the cells, cultivating the culture in an incubator, and changing half of the medium with a fresh, prewarmed neuronal medium, a scratch assay was performed on the coverslips at different “days *in vitro*” (DIV) ages. For both P6 and P17 old pups, scratch assay was performed on DIV13 and DIV20. A scratch assay is performed by using 0.1 mm tip tweezers. When angled perpendicular to the coverslip, a scratch is taken through the length in the middle of the coverslip. The groove is approximately 100  $\mu\text{m}$  wide. Each scratch assay had its matching control coverslip containing no cuts. Both cut and control coverslips were removed from the neuronal medium and fixed with 4% paraformaldehyde (PFA) containing 200 mM sucrose (both from Sigma-Aldrich) in PBS (pH 6.9) for 15 minutes, 24h or 48h after the cut was made. The fixation was performed in a separate 6-well plate, allowing the other samples to continue the incubation.

### **3.3 Immunofluorescence**

#### **3.3.1 Immunocytochemistry (ICC)**

After fixation, the cells were immediately washed three times with PBS, then incubated with 0.1 M glycine (Sigma-Aldrich) in PBS at RT, and again washed with PBS, all for 5 minutes. Coverslips were then incubated with a permeable detergent that allows further cellular antibody uptake, 0.1% Triton X-100 (Sigma-Aldrich) in PBS, for 10 minutes, followed by a 5-minute PBS wash. Blocking was achieved with 0.5% w/v BSA (Pan-Biotech) in PBS for 30 minutes. After the blocking, the coverslips were transferred to a "wet chamber" facing up and incubated with 100  $\mu$ L of primary antibody solution for at least an hour or up to two hours, in the dark. After the primary incubation, the coverslips were returned to the working wells, also facing up, and washed twice in PBS for 5 minutes. The coverslips were placed in the wet chamber again and incubated with a 100  $\mu$ L mixture of secondary antibody solution and nuclear stain 4',6-diamidino-2-phenylindole (DAPI; Thermo Fisher Scientific). Incubation was performed for at least 30 minutes or up to 2 hours, also in the dark. DAPI can be loaded in this step because it reduces ICC steps and doesn't interfere with loading of the secondary antibodies. Cells were then washed twice in PBS for 5 minutes, and once in distilled water (mQ H<sub>2</sub>O). Finally, the coverslips were mounted on glass slides previously washed with 70% ethanol, facing down. A 5  $\mu$ L drop of a mounting medium Vectashield (Vector Laboratories, Burlingame, CA, USA) was used for each mounted coverslip, which was then secured and sealed with nail polish.

#### **3.3.2 EdU staining**

EdU staining was performed using a Click-iT imaging kit (Invitrogen, Carlsbad, CA, USA). It was performed in accordance with the manufacturer's protocol. EdU solution was incorporated into culture 24 hours post cut in both cut and control culture. 10  $\mu$ M EdU working solution was prepared in combination with prewarmed neuronal medium, which was used to replace half of the medium in the cultures. EdU was left to

incubate and incorporate for another 24 hours. After fixation of the culture, through the aforementioned protocol, the incorporation of Click-iT cocktail (Click-iT reaction buffer, CuSo<sub>4</sub>, Alexa Fluor 488, reaction buffer additive) is performed after Triton X-100 permeabilization. It was incubated for 30 minutes in the dark, followed by a PBS wash, continuing the ICC protocol with a BSA block of 30 minutes and further addition of antibody solutions followed by mounting to coverslips.

### **3.3.3 Antibody solutions**

Primary antibodies and secondary antibodies used in this thesis are listed in Table 1 and Table 2, respectively. Antibody solutions for both primary and secondary incubations were prepared by diluting the antibodies in 100µL 0.5 % w/v BSA (Pan-Biotech) in PBS, according to the dilution ratios shown in Table 1 and Table 2. For some samples, the secondary antibody solution, besides DAPI, also contained the F-actin staining agent Phalloidin-iFluor 488 (Abcam, Cambridge, UK) diluted at 1:200, also in 0.5% w/v BSA (Pan-Biotech).



**Table 1** List of primary antibodies used for experiments in this work.

<b>Primary antibody</b>	<b>Host and isotype</b>	<b>Immunogen</b>	<b>Dilution</b>	<b>Manufacturer information</b>
<b><math>\beta</math>-Tubulin III (TUJ1)</b>	Monoclonal mouse IgG <sub>2a</sub>	Microtubules derived from rat brain	1:200	Biolegend Cat# 801201, RRID:AB_2313773
<b>Vimentin (vim)</b>	Monoclonal mouse IgG <sub>1</sub>	Full-length native protein	1:200	Abcam Cat# ab8069, RRID:AB_306239
<b>Vimentin (vim)</b>	Monoclonal rabbit IgG	Synthetic peptide with Human Vimentin, amino acid 400 to the C-terminus	1:200	Abcam Cat# ab92547, RRID:AB_10562134
<b>Glial fibrillary acidic protein (GFAP)</b>	Monoclonal mouse IgG <sub>1</sub>	GFAP from swine spinal cord	1:100	Sigma-Aldrich Cat# G3893, RRID:AB_477010
<b>Microtubule-associated protein 2 (MAP2)</b>	Monoclonal mouse IgG <sub>1</sub>	Bovine MAP2	1:200	Sigma-Aldrich Cat# M1406, RRID:AB_477171
<b>Ionized calcium binding adaptor</b>	Polyclonal rabbit IgG	Synthetic peptide corresponding to Human	1:200	Abcam Cat# 108539, RRID:AB_10862652

<b>molecule 1 (Iba1)</b>		Iba1 (C terminal)		
<b>S100 calcium- binding protein <math>\beta</math> (S100<math>\beta</math>)</b>	Polyclonal rabbit IgG	Synthetic peptide within Human S100 beta	1:100	Agilent Cat# Z0311, RRID:AB_10013383
<b>Apoptosis induced factor (AIF)</b>	Monoclonal rabbit IgG	KLH- conjugated synthetic peptide correspondin g to the C- terminal region of human AIF	1:100	Millipore Cat# 04- 430, RRID:AB_673048
<b>Neuron- glial antigen 2 (NG2)</b>	Polyclonal rabbit IgG	Recombinant rat Chondroitin sulphate proteoglycan 4 containing amino acids 30 to 225	1:100	Millipore Cat# AB5320, RRID:AB_91789
<b>Growth- associate d protein 43 (GAP43)</b>	Monoclonal rabbit IgG	Synthetic peptide (Info not available)	1:100	Abcam Cat# ab75810, RRID:AB_1310252

**Table 2** List of secondary antibodies used for experiments in this work

<b>Secondary antibody</b>	<b>Host and isotype</b>	<b>Immunogen</b>	<b>Dilution</b>	<b>Conjugation</b>	<b>Producer Cat # RRID</b>
Goat anti-rabbit IgG (H+L)	Goat polyclonal IgG	Not Available	1:300	Alexa Fluor® 647	Abcam, ab150083, AB_2714032
Goat anti-mouse IgG <sub>2a</sub> (H+L)	Goat polyclonal IgG <sub>2a</sub>	Mouse IgG <sub>2a</sub>	1:300	Alexa Fluor® 555	Thermo Fisher Scientific, A21137, AB_2535776
Goat anti-mouse IgG1	Goat polyclonal IgG1	IgG gamma 1	1:300	Alexa Fluor® 488	Thermo Fisher Scientific, A21121, AB_2535764

### 3.4 Fluorescence microscopy

Immunofluorescence-stained samples were visualized and analysed with an Olympus IX83 inverted fluorescent microscope (Olympus), equipped with fluorescence optics mirror units (Table 3), and differential interference contrast (DIC). Images from the microscope were obtained with a Hamamatsu Orca R2 CCD camera (Hamamatsu Photonics, Hamamatsu, Japan) and CellSens software (Olympus). Objectives that were used were 10x with 0.3 numerical aperture (NA); air, 20x with 0.5 NA; air and 60x with 1.42 NA; oil immersion. Additional 1.5x and 2x magnifications were used to enlarge cell visualization.

**Table 3** List of filter cubes in Olympus IX83 that were used for fluorescence microscopy (Chroma, Irvine, CA, USA). Filter and mirror units in nm.

	<b>Unit</b>	<b>Excitation filter</b>	<b>Emission filter</b>	<b>Dichromatic mirror</b>
<b>Ultraviolet Excitation</b>	U-FUNA	360-370	420-460	410
<b>Blue Excitation</b>	U-FBW	460-495	510IF	505
<b>Green Excitation</b>	U-FGW	530-550	575IF	570
<b>Far-Red Excitation</b>	Cy5	590-650	663-738	660

To reach the optimal focal point for each image, Z stacking was performed, with different spacing depending on the magnification, with at least 10 frames per sample and the suggested slice spacing. To optimize images with only one focal plane, Z offset was performed to reduce the background noise and calibrate the optimal focal plane for each emission channel.

Image processing, including extended focus image (EFI) and deconvolution was performed using CellSens software (Olympus). Image analysis, including measurement of growth cones was performed using ImageJ (FIJI; National Institutes of Health, WI, USA).

### **3.5 Data analysis**

At least three randomized locations within the sample were used to obtain data for this work. Cell counting for separate markers and image compositions was performed using ImageJ (FIJI; National Institutes of Health, WI, USA) plugin extension CellCounter.

GraphPad Prism 9 (GraphPad Software Inc., San Diego, CA, USA) was the software of choice for performance of statistical analysis. Three data

groups were compared through two-way ANOVA with Geisser-Greenhouse correction, assuming differences weren't equally variable, with Tukey correction for multiple comparisons. Unpaired t-tests were used to statistically compare two normally distributed data sets, with Welch's correction, assuming SDs were not equal. Level of significance was set at  $p < 0.05$ .

APA (American Psychological Association) was the choice of p value indication style. Accepted level of significance was  $p < 0.05$ .  $p \geq 0.05$  (not significant; ns),  $.05 > p > .01$  (significant; \*),  $0.01 > p > 0.001$  (very significant; \*\*),  $< 0.001$  (very significant; \*\*\*).

## **4 RESULTS**

### **4.1 Primary neuronal cell cultures from *Monodelphis domestica* cortexes**

In this work, primary neuronal cell cultures obtained from *Monodelphis domestica* at two different development ages, P6 and P17. Cultures had a good survival rate, allowing the cells to be maintained up to a month in an incubator at 32 °C, with relative humidity set at 95% and 5% CO<sub>2</sub>. The neuronal cultures were analysed up to DIV20 for both P6 and P17 opossums. These cultures have the ability to produce developmental processes *in vitro*, including GC sprouting, dendritic and axonal growth, network formation, and others <sup>36</sup>.

### **4.2 Cellular identification and culture maturation within different age groups**

#### **4.2.1 Markers for cellular identification**

*M. domestica* share high protein homology with other mammals but very few commercially available antibodies were previously tested on these cultures. The complete list of neuronal and glial markers used in this thesis is shown in Table 1.

#### **4.2.2 Neurogenesis and neuronal identification using ICC**

Early growing of neurites, GC sprouting, and further neuronal development was observed using primary cultures prepared from P6 cortex at DIV1, DIV5 and DIV13. Neuronal maturation was observed at DIV20. P6 is the optimal age for investigating the early steps of cortical development in opossums, which complete their neurogenesis by P16 <sup>34</sup>.

At DIV1, two different combinations of markers were tested. To stain neurite growth and detect an early phase of neuronal differentiation, cytoskeletal neuronal marker  $\beta$ -Tubulin III (TUJ1) was used.  $\beta$ -tubulin III is classified as a class III member of the  $\beta$ -tubulin proteins, and a neuron-specific isoform.  $\beta$ -tubulins are one of the components of microtubular

network within the cell. Expression of TUJ1 is mainly observed in the initial phases of neuronal differentiation, in comparison with other classes of tubulin, which are mainly involved in cellular processes such as mitosis<sup>37</sup>. The signal is localized in the cell body, dendrites, and axons. To characterize the cellular cytoskeleton and detect GC sprouting, structures rich with peripheral actin, a fluorescent probe phalloidin (PHALL) that binds filamentous (F) actin was used. These two markers were used in both samples. To further characterize the cell composition, vimentin (vim), which at early development is expressed in radial glia and immature astrocytes, was used in one sample. Vimentin is a type III intermediate filament protein found in developing astrocytes, and it is upregulated in astrocytes undergoing astrogliosis<sup>38</sup>. Growth-associated protein 43 (GAP43) was used as a neuron-specific marker and a major axon terminal and GC component<sup>39</sup>. GAP43 is a presynaptic phosphoprotein localized on the inner surface of the plasma membrane of growing axons<sup>39</sup>. At least three randomized visual fields per sample were chosen, and cells were counted. Each marker's value within the total sample size (n, number of counted cells) is computed as mean  $\pm$  standard deviation.

At DIV1 (Figure 7),  $60.55 \pm 9.65\%$  (n=343) of the cells within the sample were positive for the neuronal marker TUJ1 (TUJ1+), followed by vim-positive cells (vim+;  $29.54 \pm 8.01\%$ , n=343). Vim and TUJ1 are mutually exclusive markers, yet at this developmental stage, cells positive for both markers were detected as well (TUJ1+/vim+;  $14.29 \pm 1.58\%$ , n=343). Cell debris as well as fragmented and pyknotic cell nuclei observed with DAPI were not taken into account for counting.

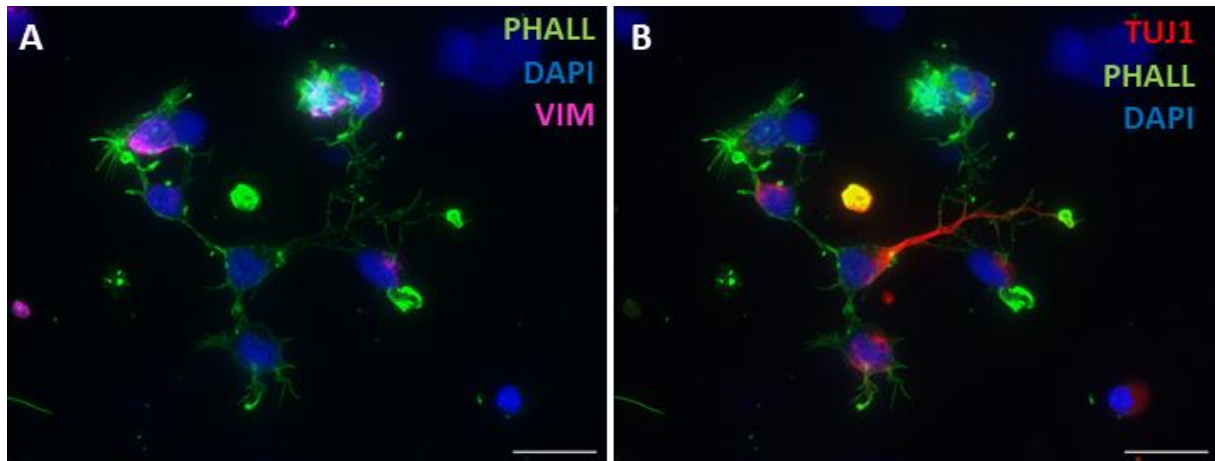


**Figure 7** Primary neuronal cells culture obtained from P6 opossum pup fixed at DIV1 and stained for  $\beta$ -tubulin III (TUJ1; red), filamentous (F) actin (PHALL; green), nuclei (DAPI; blue) and intermediate filaments (vim; magenta). **(A)** Magnified inset of vim-stained cells **(B)** Magnified inset of TUJ1 stained cells. 60x and 1.4 NA oil-immersion objective; scale bar 20  $\mu$ m.

At DIV1, TUJ1+ neurons started sprouting their GCs trying to find contact with neighbouring cells to form synapses (Figure 8). Sprouting is depicted by a strong phalloidin staining signal (Figure 8A, green arrows). Vim+ cells indicate non-differentiated immature precursors of CNS cells, as they express the intermediate filament vimentin. Some cells that might have begun their differentiation into neuronal cells express TUJ1 and show very weak vimentin stain (Figure 8A, B and E, red arrow), suggesting that they are completing vimentin downregulation upon induction of neuronal differentiation. These TUJ1+/vim+ cells have a round shape with actin-rich short protrusions around the cell body without well-defined neurites. Moreover, vimentin stain in TUJ1-negative (TUJ1<sup>-</sup>) cells is visibly stronger.



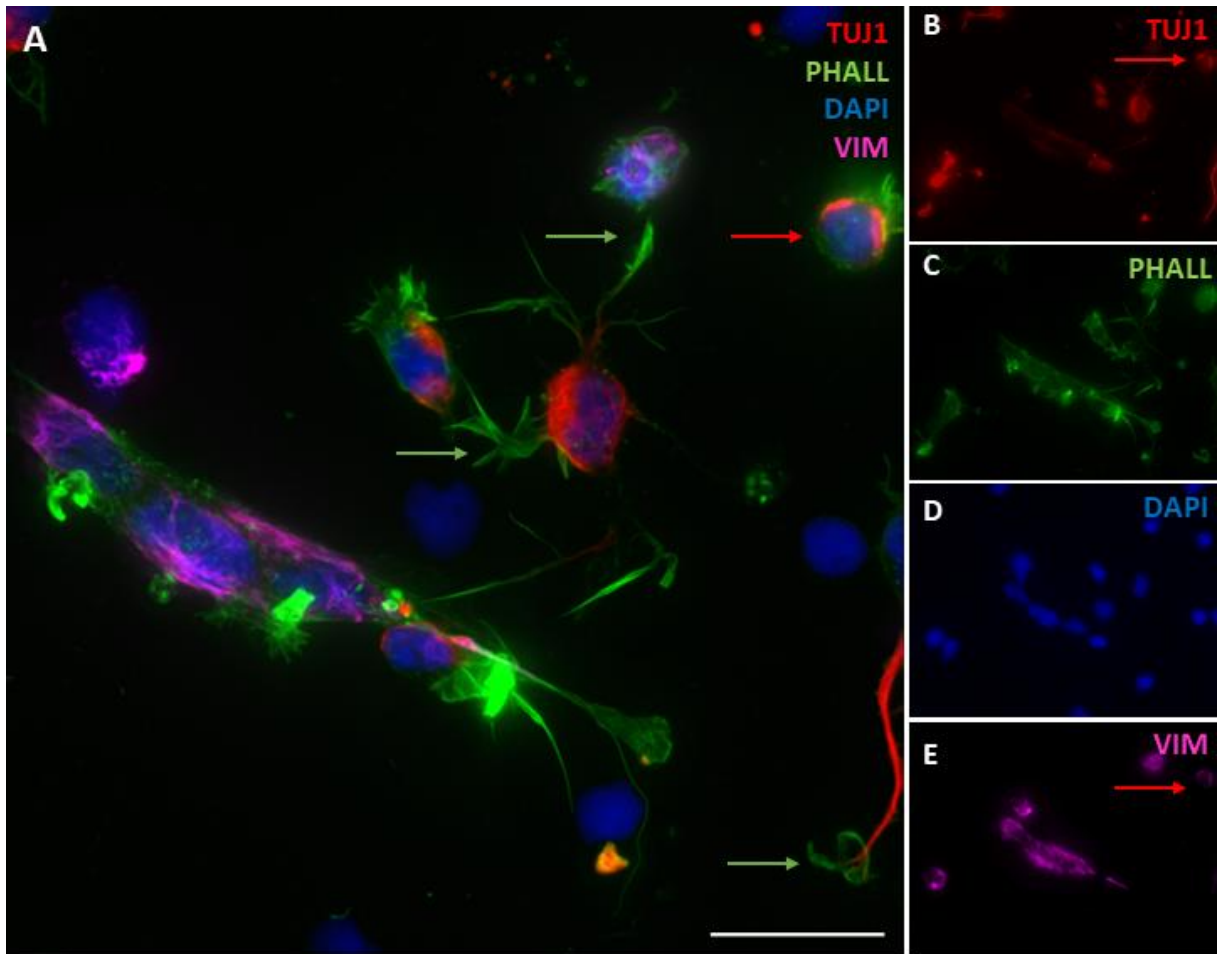


**Figure 8 (A)** Neuronal cell culture prepared from P6 opossums, fixed at DIV1, stained with TUJ1 (red), phalloidin (PHALL, green), DAPI (blue) and anti-vimentin antibody (vim, magenta), and imaged using 60X and 1.4 NA oil-immersion objective. Green arrows indicate phalloidin-rich sprouting GCs of a developing neuron. Red arrow indicates a cell that is starting its differentiating process into a TUJ1+ neuron. **(B)** Neuronal stain TUJ1 (red). **(C)** Filamentous F-actin staining with phalloidin (green). **(D)** Nuclear stain DAPI (blue). **(E)** Vimentin stain (magenta). Scale bar 20  $\mu$ m.

A second sample tested for GAP43 in combination with TUJ1, phalloidin and DAPI showed several problems (Figure 9). First of all, TUJ1-positive cells were detected in lower quantities ( $52.99 \pm 11.98\%$ ;  $n=302$ ) than expected at DIV1<sup>35</sup>. GAP43-positive cells were identified ( $56.93 \pm 13.44\%$ ;  $n=302$ ) in both neurons (GAP43+/TUJ1+;  $40.10 \pm 9.48\%$ ;  $n=302$ ) and non-neuronal, RGC-like cells (GAP43+/TUJ1<sup>-</sup>; Figure 9, white arrow). However, during imaging, GAP-43 required a higher exposure time to obtain the signal (1.99 s, compared to other channels which required exposure time between 100-300ms). The higher exposure time for GAP43 resulted in a punctuated background signal as well. Moreover, DAPI stain

showed smeared nuclei indicating that enhanced cell damage occurred during dissociation and plating. Therefore, this particular experiment should be repeated and the GAP43 expression in these cultures should be further validated<sup>35</sup>.

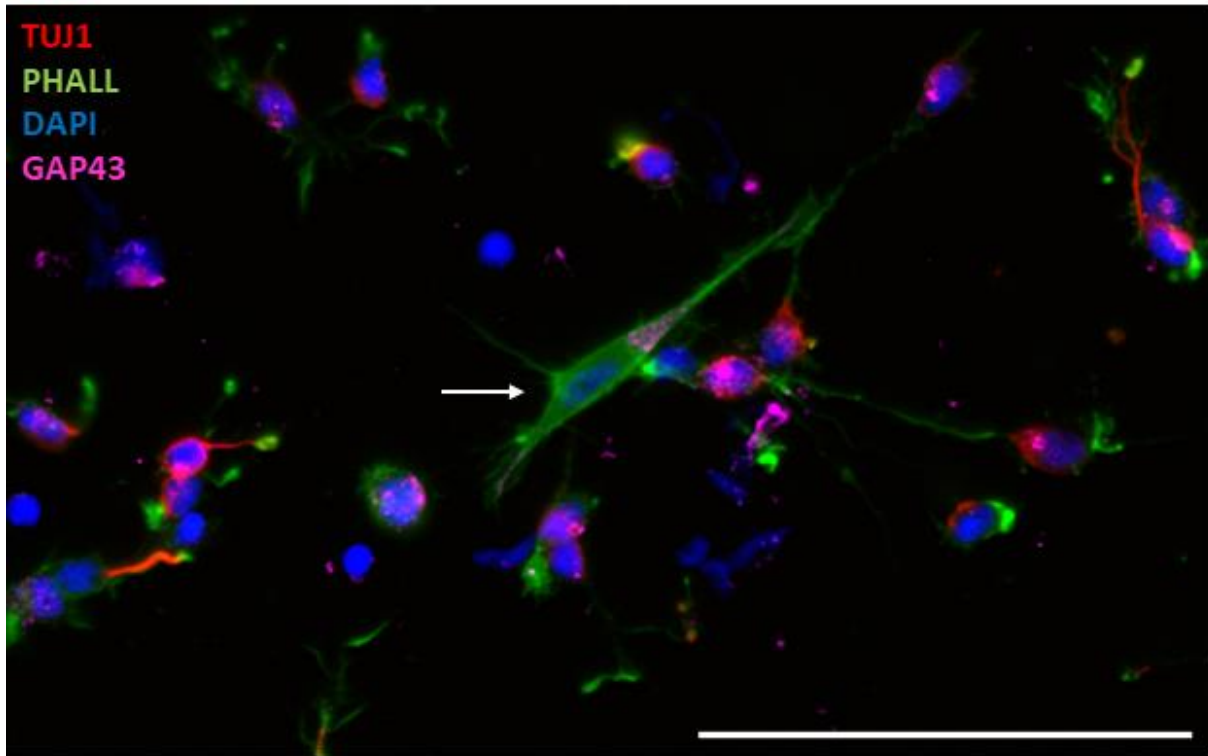


**Figure 9** Primary neuronal cells obtained from P6 opossum pup fixed at DIV1 and stained for following markers:  $\beta$ -tubulin III (TUJ1; red), filamentous (F) actin (PHALL; green), nuclei (DAPI; blue) and growth associated protein (GAP43; magenta). An RGC-like cell with a GAP43+ signal is labelled with an arrow. Smeared DAPI stain indicates damage within sample. Scale bar 100  $\mu$ m.

We next analysed the *in vitro* cell maturation of the same culture preparation (P6 cortex) at DIV5 (Figure 10). At DIV5, extensive cell outgrowth was observed with phalloidin staining (Figure 10A). TUJ1+ cells were the most abundant cells, with their percentage being at the highest level ( $84.05 \pm 7.61\%$ ;  $n=123$ ), followed by vim+ cells ( $17.21 \pm 9.75\%$ ;  $n=123$ ). Only a fraction of cells tested double-positive for TUJ1 and vim ( $11.35 \pm 3.33\%$ ;  $n=123$ ). Neurite branching, (extensive outgrowth of collateral processes and connection with neighbouring neurons) occurred, confirming the *in vitro* neuronal network formation.

At DIV13 (Figure 10B), further *in vitro* cell maturation was confirmed. Neuronal number decreased, but still yielded the highest percentage for TUJ1+ ( $44.73 \pm 7.50\%$ ;  $n=389$ ), followed by vim+ cells ( $35.99 \pm 12.15\%$ ;  $n=389$ ). Double positive cells were present in lower quantities ( $4.98 \pm 0.92\%$ ;  $n=389$ ), which could indicate cellular overlapping or persistence of double-positive cells. The results of cell counting are shown in Figure 10C.

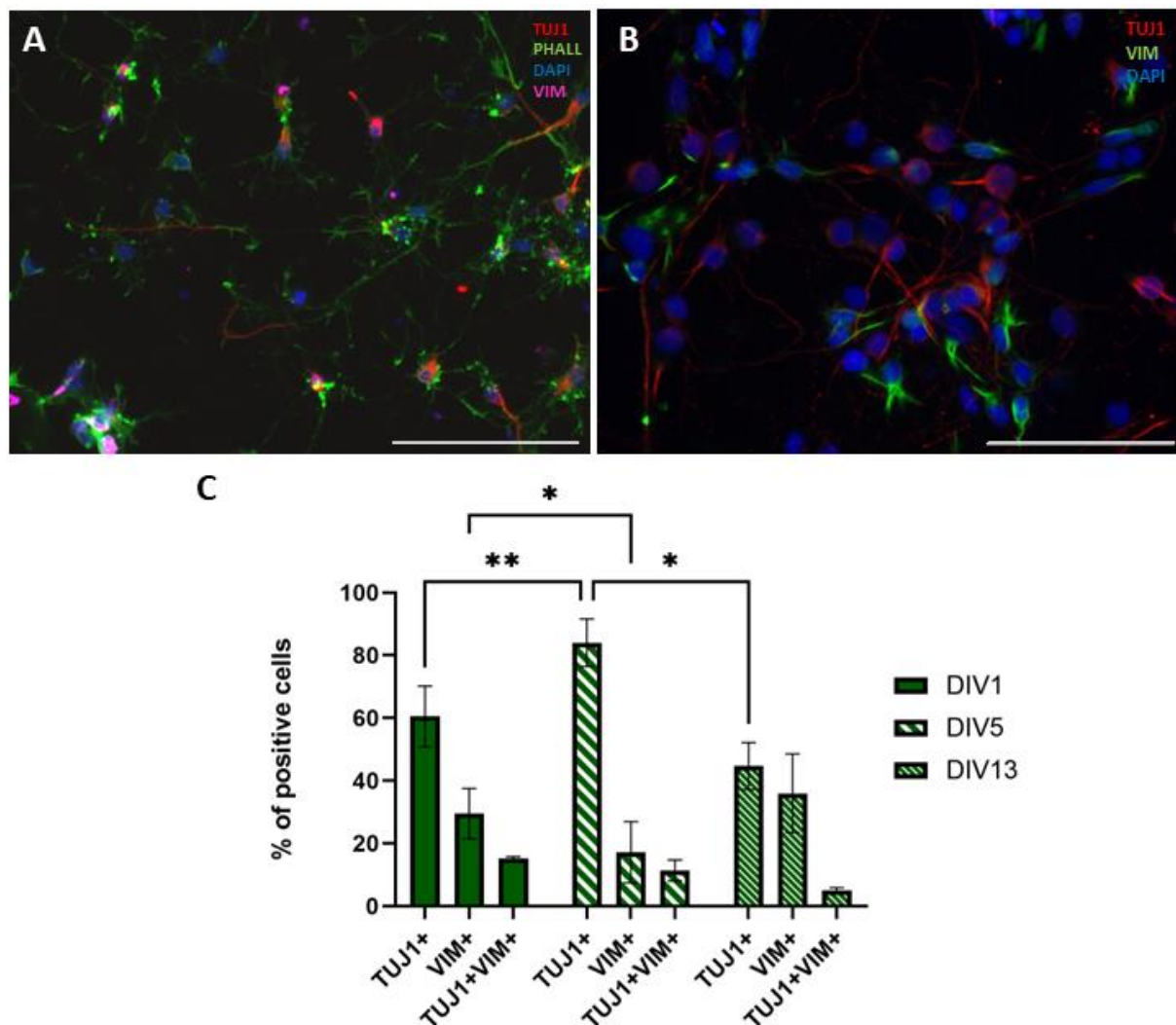


**Figure 10** Primary neuronal cell cultures obtained from P6 opossum pup were fixed and stained at **(A)** DIV5;  $\beta$ -tubulin III (TUJ1; red), filamentous (F) actin (PHALL; green), nuclei (DAPI; blue) and vimentin (vim; magenta), and **(B)** DIV13;  $\beta$ -tubulin III (TUJ1; red), vimentin (vim; green), nuclei (DAPI; blue). Scale bar for **(A)** 100  $\mu$ m; **(B)** 50  $\mu$ m (2x magnification of 20x). **(C)** Two-way ANOVA with Geisser-Greenhouse correction, and Tukey's multiple comparisons test. TUJ1+ DIV1 vs. DIV5,  $p = .005^{**}$ , DIV1 vs. DIV13,  $p = .079^{ns}$ ; DIV5 vs. DIV13,  $p = .01^{*}$ . vim+ DIV1 vs. DIV5,  $p = .013^{*}$ ; DIV1 vs. DIV13,  $p = .409^{ns}$ ; DIV5 vs. DIV13,  $p = .055^{ns}$ .

Lastly, to identify mature neurons within a culture, their presence is tested with microtubule-associated protein-2 (MAP2). MAP2 belongs to a family of proteins that stabilize neuronal shape by encouraging microtubule synthesis. It is a neuron-specific protein predominately localized in the dendrites of mature neurons<sup>40</sup>. Mature neurons were set to be identified in DIV20, since neurogenesis in opossums should be completed by P16<sup>34</sup> (Figure 11). As expected, MAP2-stained neurons have shown colocalization with TUJ1+ neurons, mainly in the soma and thicker neurites, given MAP2 is a somatodendritic marker, while TUJ1+/MAP2-thin neurites marked axons.

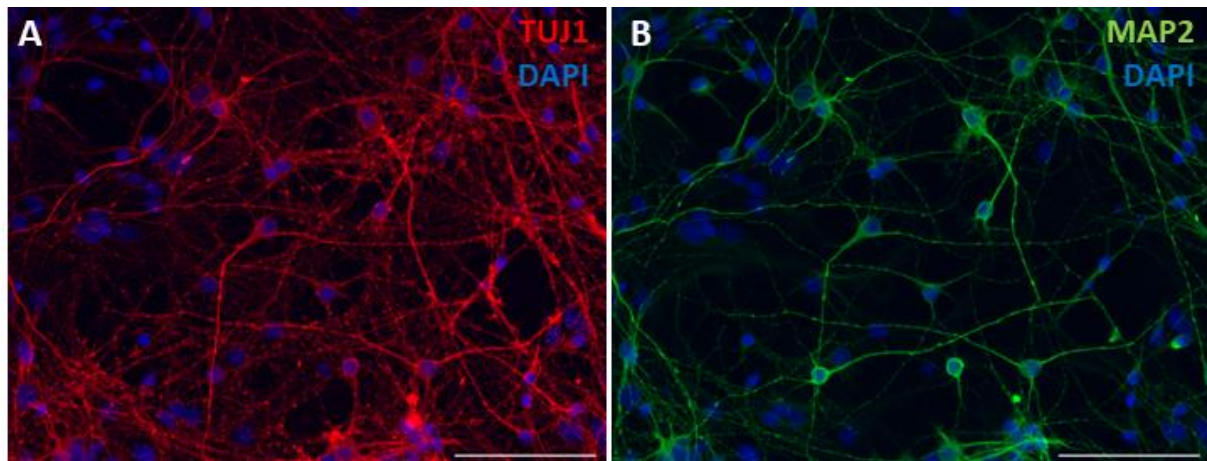


**Figure 11** Expression of **(A)** immature neuronal marker  $\beta$ -tubulin III (TUJ1; red) and **(B)** mature neuronal marker microtubule-associated protein-2 (MAP2; green) with nuclear marker (DAPI; blue). Both images represent the same position within the sample obtained from P6 opossum fixed at DIV20. Scale bar 100  $\mu$ m.

#### 4.2.3 Identification of glial cells

Besides neuronal cells, one of the goals of interest was to characterize non-neuronal cells within the primary cortical cultures derived from opossums. Specifically, the goal was to identify astrocytes within the samples and investigate their *in vitro* maturation. Glial fibrillary acidic protein (GFAP) is an astrocytic marker that can help depict the morphological features of an astrocyte, whether it is protoplasmic or fibrous, and help to quantify mature astrocytes. GFAP is a highly expressed component of the astrocytic cytoskeleton, along with actin and

vimentin. It helps define shape and mobility within astrocytes. In comparison to vimentin, GFAP is upregulated in mature astrocytes and progressively replaces vimentin towards the end of gestation in differentiated astrocytes<sup>41</sup>. Moreover, increased GFAP immunoreactivity showcases activated astrocytes, correlating with neural damage <sup>42</sup>. GFAP expression was analysed at DIV5 and DIV13 in P6 opossums, in combination with vimentin.

At DIV5 (Figure 12A),  $35.89 \pm 6.73 \%$  (n=120) of cells expressed vim and  $28.78 \pm 3.30\%$  (n=120) expressed GFAP. Almost all cells that were GFAP+ also expressed vim (GFAP+/vim+;  $81.05 \pm 6.82\%$ , n=44). At DIV13 (Figure 12B), the sample was additionally tested for S100 $\beta$ . S100 $\beta$  is a calcium-binding protein, a member of the S100 family of proteins. They are localized in the cytoplasm and associated with membranes as well as the cytoskeleton. They are found in astrocytes, and their levels are elevated in astrogliosis. Besides astrocytes, S100 $\beta$  can also be found in RGC of the cerebellum and the subventricular zone <sup>43</sup>. However, in our experimental conditions, the staining wasn't specific for GFAP+ astrocytes only, showing a signal in the majority of cells, including those with neuron-like morphology. Therefore, only GFAP was quantified in P6 opossum culture at DIV13, with GFAP+ cells accounting for  $32.37 \pm 9.15\%$  (n=267). The majority of the astrocytes that were observed were protoplasmic in shape.

In the P6 opossum culture at DIV20, as the culture further matured, vimentin allowed identification of both fibrous (Figure 12C) and protoplasmic (Figure 12D) astrocytes in the sample.



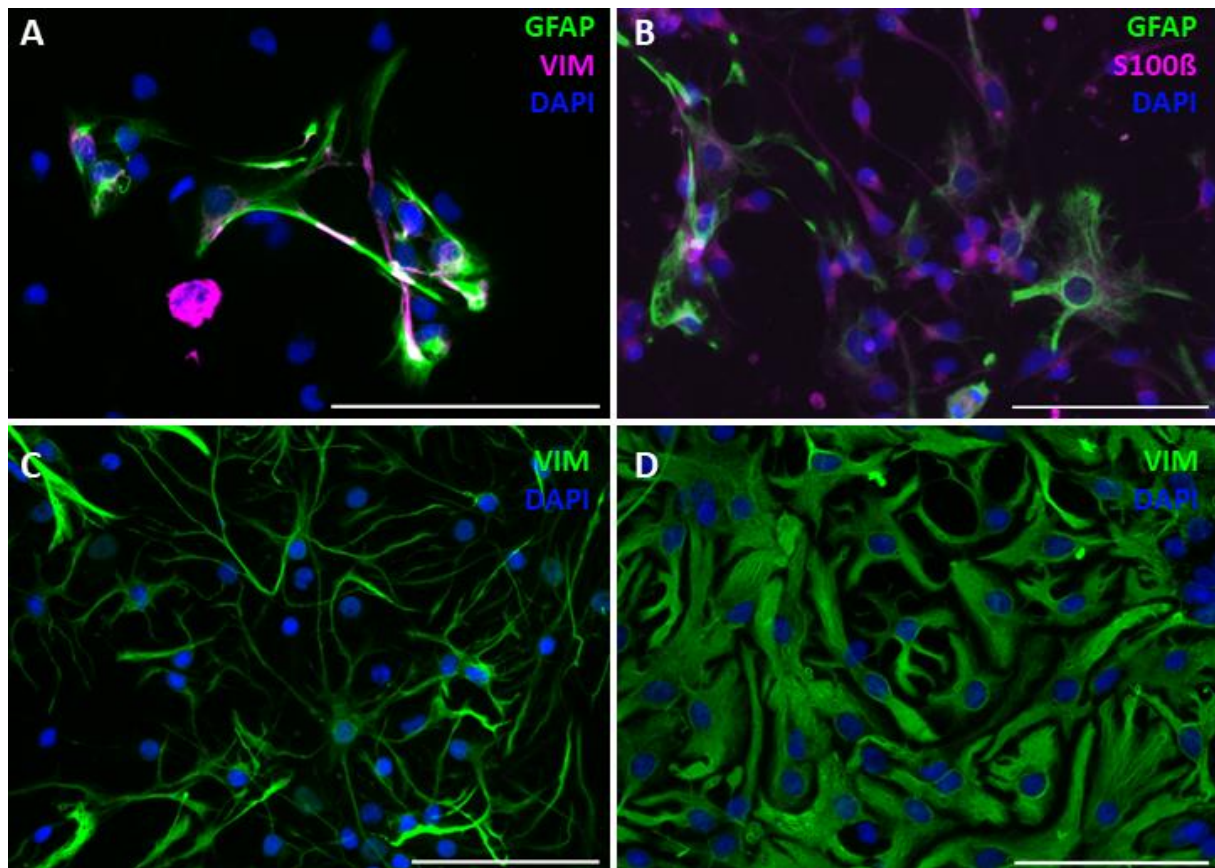


**Figure 12** **(A)** P6 opossum cortical cultures fixed at DIV5 and stained for glial fibrillary acidic protein (GFAP; green), vimentin (vim; magenta) and nuclei (DAPI; blue). **(B)** DIV13 culture stained for glial fibrillary acidic protein (GFAP; green), calcium binding protein (S100B; magenta) and nuclei (DAPI; blue). Representative fields of **(C)** fibrous and **(D)** protoplasmic astrocytes fixed at DIV20 and stained for vimentin (vim; green) and nuclei (DAPI; blue). Scale bar 100  $\mu$ m.

To further characterize the culture composition, the samples were stained with markers to detect other glial cells apart from astrocytes. Specifically, two markers were tested: ionized calcium binding adaptor molecule 1 (Iba1) and neuron-glial antigen 2 (NG2). Iba1 is a calcium-binding protein specific for microglia and macrophages. It is involved in phagocytosis in microglia that are activated <sup>44</sup>. NG2 is a chondroitin sulphate proteoglycan found in oligodendrocyte progenitor cells. Iba1 was tested on both P6 and P17 cortical cultures, at DIV13 and DIV20, respectively. The marker yielded no signal. NG2 was tested for oligodendrocyte precursors' presence in P6 cortical cultures at DIV20. The marker yielded a very low signal and, given the high density of cellular network, it was not quantified (Figure 13A, magenta arrows). Interestingly, at DIV20, staining with phalloidin on separate samples of the same P6 cortical culture showed

highly branched morphology of some cells, distinct from both neurons and glia (TUJ1<sup>-</sup>/vim<sup>-</sup>, Figure 13B, C). Further experiments with additional markers are required to identify these non-neuronal cells.

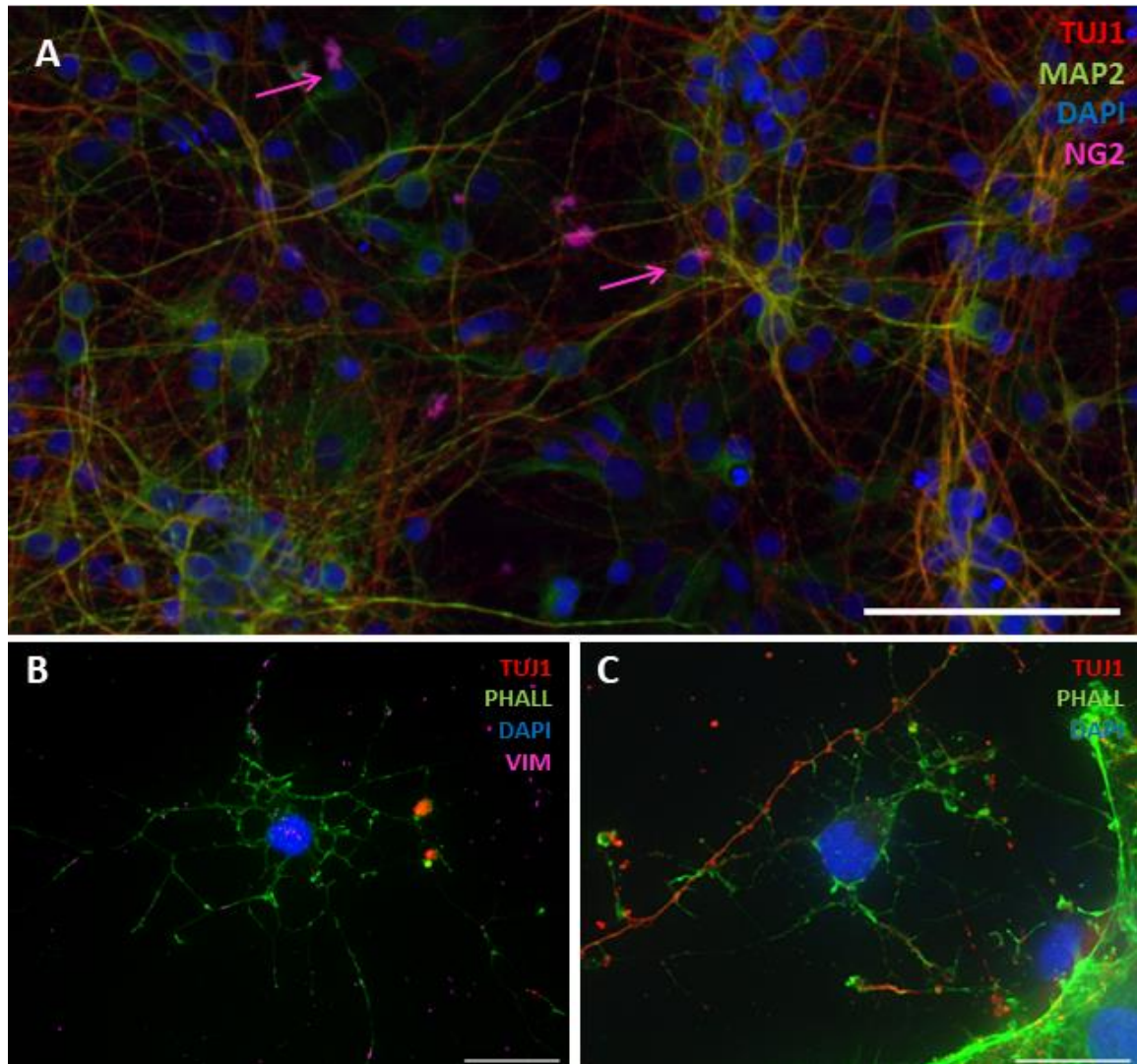


**Figure 13** (A) Fixed sample of P6 cortical culture at DIV20, inspected for the presence of oligodendrocyte precursors, by staining for neuro-glial antigen 2 (NG2; magenta). Purple arrows indicate potential cells that yield positive NG2 signal. The sample was also stained for  $\beta$ -tubulin III (TUJ1; red), microtubule-associated protein-2 (MAP2; green), and nuclei (DAPI; blue). Scale bar 100  $\mu$ m. TUJ1<sup>-</sup>/vim<sup>-</sup> cells found at DIV20, stained for (B)  $\beta$ -tubulin III (TUJ1; red), F-actin (PHALL; green), nuclei (DAPI; blue) and vimentin (vim; magenta), and (C)  $\beta$ -tubulin III (TUJ1; red), F-actin (PHALL; green), nuclei (DAPI; blue). Scale bar 20  $\mu$ m.

### **4.3 Cellular behaviour and the regenerative capacity of primary cell cultures upon an induced injury *in vitro***

Since *M. domestica* are born at a very immature state, neuronal cell cultures derived from their cortices not only retain the ability to perform neuronal development *in vitro*, but they also have the ability to regenerate their axons after *in vitro* injury <sup>45</sup>. In addition to neuronal regeneration, these cultures allow the expansion of the research by looking into glial cell activation (astrocytes in particular). Regeneration potential was inspected through a “scratch assay”, an artificial injury approximately 100 µm wide produced by tweezer tip along the central line of the coverslip. Essentially, the cut disrupts the neuronal network, mimicking primary injury – shearing and transection. The cultures were then fixed either 24h or 48h post-injury and immunostained. The scratch assay was performed in both P6 and P17 opossum cell cultures at the same point, DIV13 and DIV20 respectively.

An example of injury site of P6 culture at DIV20 is shown in Figure 14. Samples were fixed and stained 24 hours after injury. TUJ1 staining showed numerous neurons present in the culture almost three weeks after plating. At the injury site, after 24 hours, growing axons that extend to the cut site can be observed, stained with TUJ1. They sprout perpendicularly to the cut site, with a change of growth orientation to parallel as they reach the central region, presumably containing the groove made by the tweezer tip, affecting their growth orientation. After the axons reach the groove, they continue to connect perpendicularly with the neurons on the other side. Growing neurites are characterized by stronger F-actin signal at their tips, indicating the formation of new GCs, if the neurites are capable of growth across the cut site, or RBs, if the growth is halted. Moreover, small-sized DAPI+ fragments were observed in the area around the cut, indicating that cellular death had occurred following the injury.



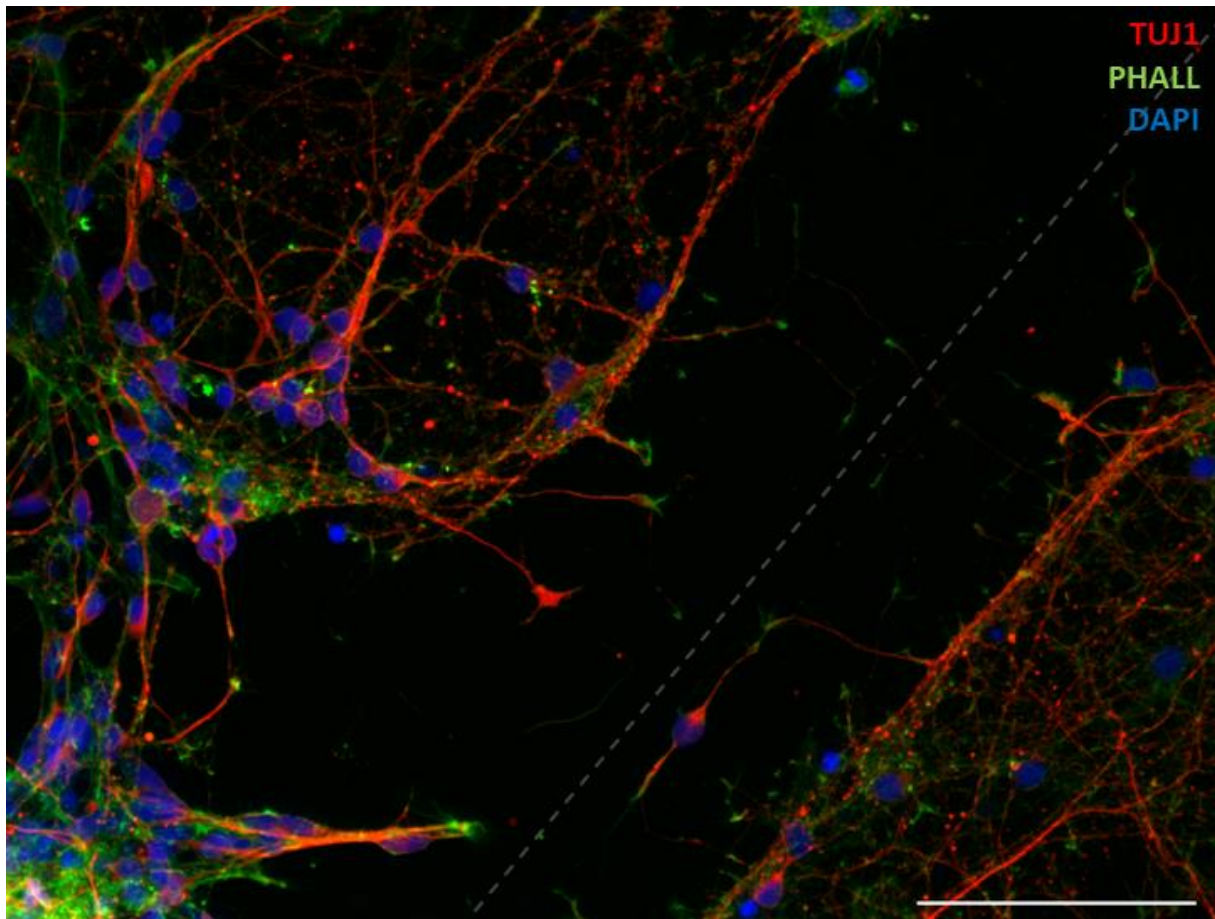


**Figure 14** Injured region in P6 cortical culture at DIV20, 24 hours after performing a "scratch-assay", stained for  $\beta$ -tubulin III (TUJ1; red), filamentous (F) actin (PHALL; green), and nuclei (DAPI; blue). Dashed line represents the cut site. Scale bar 100  $\mu$ m.

In response to the injury, astrocytes undergo astrogliosis and shift from the resting to the reactive phenotype, initializing the defence mechanism by generating a glial scar and closing the gap. They change their morphology by increasing in size, hyperbranching and extending their processes, reducing the gap made by the cut. Reactive astrocytes in P6 cortical culture were fixed at DIV20, 24 hours after the cut are shown in Figure 15. Astrocytes near the cut region transform into their activated state, which is depicted by elongated processes that are polarized in the direction of the cut groove (Figure 15A). These astrocytes form so-called palisades. Astrocytes distant from the injury site don't show the reactive morphology and their processes extend in all directions (Figure 15B). Polarized, elongated astrocytic processes are not the only ones enclosing the gap, as they give sense of direction for axonal extension across the

cut (Figure 15A, squared inset). TUJ1-labelled neurons elongate through the cut trying to connect with other side (Figure 15C).

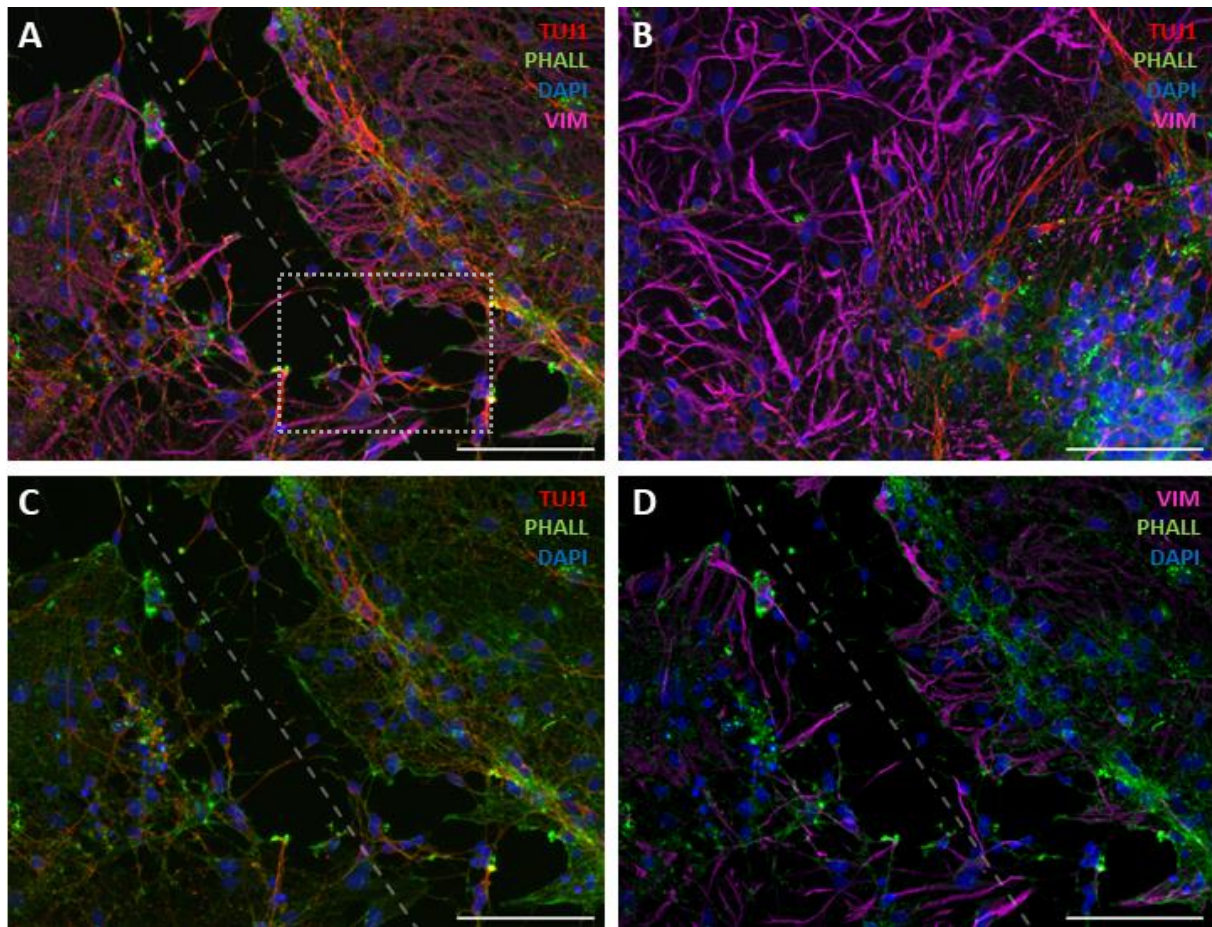


**Figure 15** P6 cortical culture fixed at DIV20, 24 hours post cut, and stained for  $\beta$ -tubulin III (TUJ1; red), filamentous (F) actin (PHALL; green), nuclei (DAPI; blue), and vimentin (vim; magenta). **(A)** Representative field showing activated astrocytes forming palisades with their polarized processes. Dashed square indicates astrocytic guidance for neurons crossing the lesion site. **(B)** Control sample with resting astrocytes. **(C)** Neurons with elongated axons make connections through the cut site. **(D)** vim staining showing activated astrocytes palisades in the proximity of the cut. Dashed line represents the cut direction. Scale bar 100  $\mu$ m.

Astrocytes do not only extend their polarized processes at the cut site, but also migrate to, and through the cut site. A case of migrating astrocytes with a hypertrophic morphology has been observed in P17 cortical culture at DIV13 (Figure 16A). F-actin was strongly expressed in the migrating cells, with actin cytoskeleton organized in a dense network of filaments throughout the cell body, as well as in protruding, filopodia-like extensions at the cell periphery (Figure 16B, C). Vimentin staining has again shown to be unsuccessful, as it yields fragmented signals.



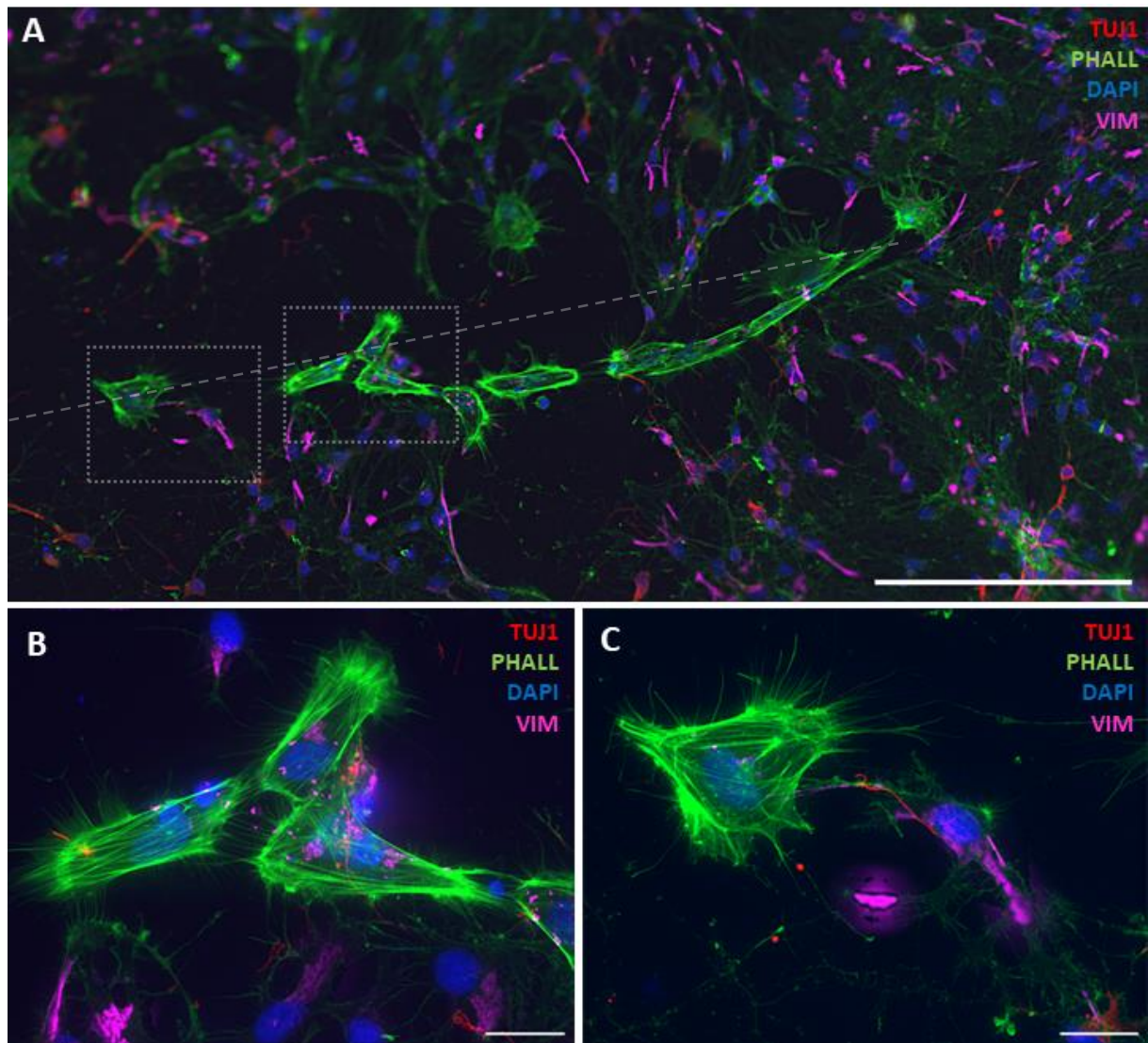


**Figure 16** P17 cortical culture fixed at DIV13, 24 hours post cut, and stained for  $\beta$ -tubulin III (TUJ1; red), filamentous (F) actin (PHALL; green), nuclei (DAPI; blue), and vimentin (vim; magenta). **(A)** Migrating astrocytes in the cut site with reactive morphology and strong PHALL signal. Dashed line represents the cut. Scale bar 200  $\mu$ m. **(B, C)** Higher magnification image of squared insets from migrating astrocytes in (A) using 60x and 1.4 NA oil-objective. Scale bar 20  $\mu$ m.

#### 4.3.1 Cellular fate upon injury: proliferation and death

To test whether cells undergo division and proliferate in response to injury, DNA synthesis was detected by utilizing 5-ethynyl-2'-deoxyuridine (EdU), which is incorporated into DNA as a thymidine analogue. EdU has a replaced methyl group at the 5-position of the pyrimidine ring with an alkyne group. This terminal alkyne group reacts with fluorescent azides and is highly incorporated thanks to its ability to easily penetrate through tissues <sup>46</sup>. EdU incorporation was tested in P17 cortical culture, stained

with EdU 24 hours post cut, and fixed 48 hours post cut at DIV20. The signal was observed and quantified in three randomised fields as control (without cut) and cut samples. The control sample (Figure 17A) yielded a higher number of EdU positive cells (EdU+<sup>CTRL</sup>;  $10.78 \pm 3.87\%$ ;  $n=1031$ ), while the cut sample (Figure 17B) showed lower percentages (EdU+<sup>CUT</sup>;  $7.98 \pm 1.41\%$ ;  $n=602$ ). The results were statistically analysed with an unpaired t-test, with results not being significantly different ( $p=.303$ ; Figure 17C). Elevated pyknotic DAPI signal in cut sample could affect total cell number, in addition to reduced cell density caused by the cut itself.

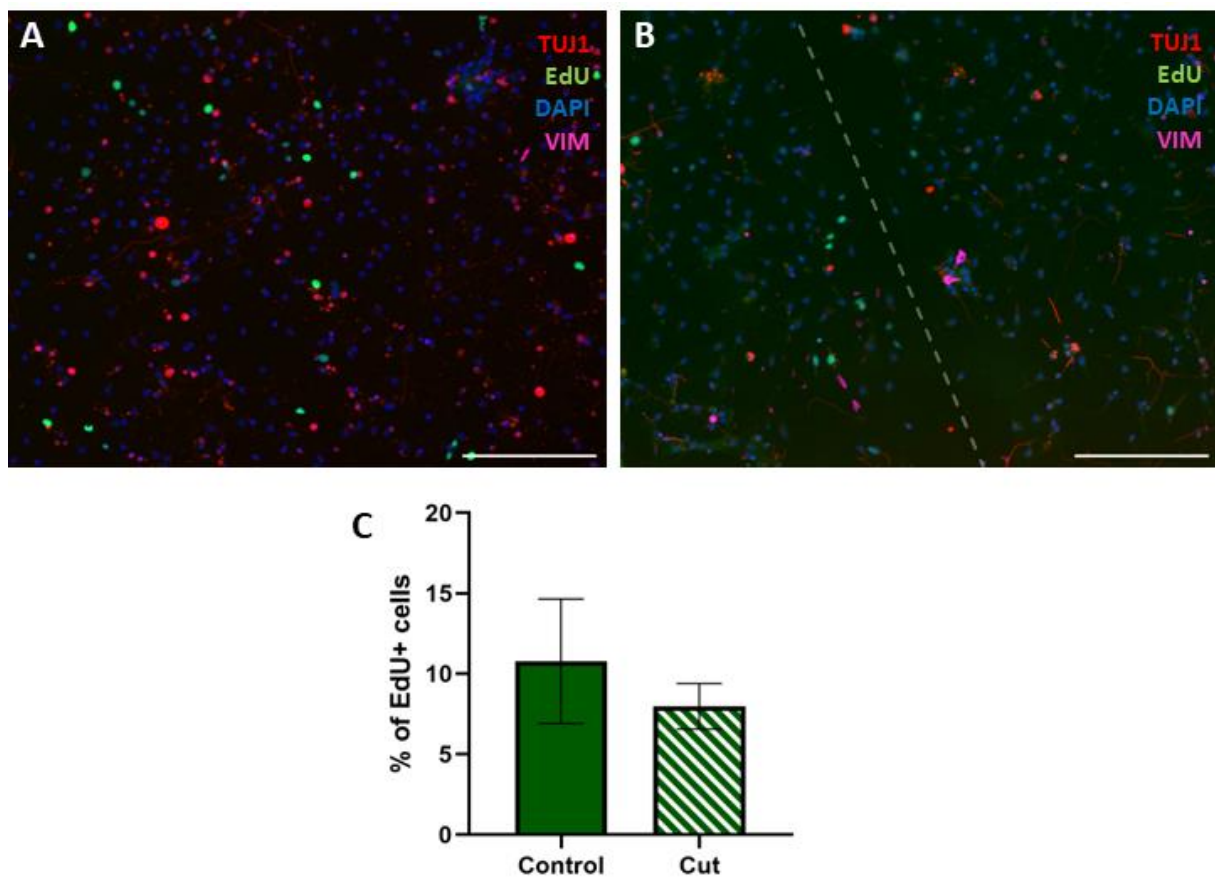


**Figure 17** P17 cortical culture fixed at DIV20, 48 hours post cut, and stained for  $\beta$ -tubulin III (TUJ1; red), 5-ethynyl-2'-deoxyuridine 24 hours after cut (EdU; green), nuclei (DAPI; blue), and vimentin (vim; magenta). **(A)** Control sample. **(B)** Cut sample. Dashed line represents cut site. Scale bar 200  $\mu$ m. **(C)** Comparison of EdU+<sup>CTRL</sup> vs. EdU+<sup>CUT</sup>. Unpaired t-test with Welch's correction. Control vs. cut  $p = .303$ ; not significant. Data is given as mean  $\pm$  SD.

We can assume that in addition to reduced proliferation, cell death could be observed through morphological changes. Pyknosis is one of the processes of programmed cell death, resulting in irreversible condensation

of chromatin, followed by fragmentation of the nucleus, also known as karyorrhexis. This can be observed with DAPI staining localized in small-sized nuclear fragments (Figure 18A). Besides pyknotic bodies, cellular death can be observed through blebbing, irregular bulges of the membrane that ultimately form apoptotic bodies loaded with discharged molecules (Figure 18B).

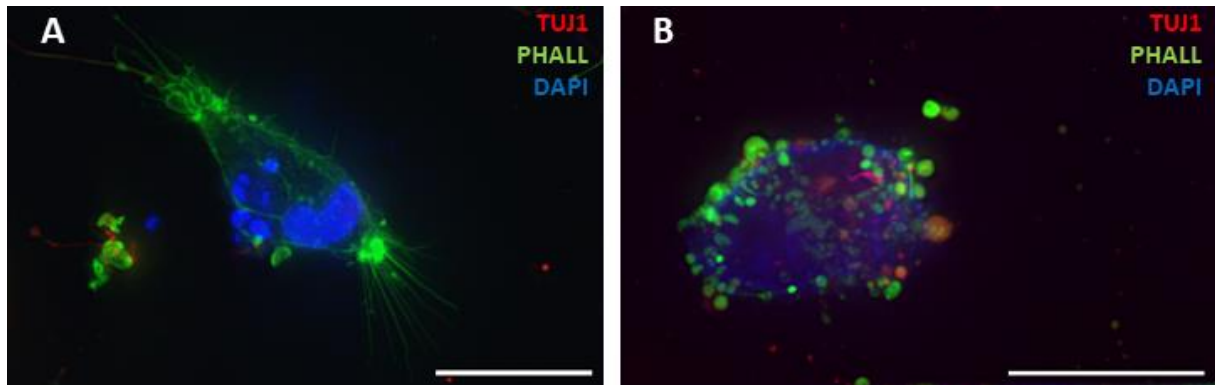


**Figure 18 (A)** Insets of karyorrhexis, nuclear fragmentation, presumably phagocytosed by an astrocyte and **(B)** cell blebbing. Samples are stained for  $\beta$ -tubulin III (TUJ1; red), filamentous (F) actin (PHALL; green), nuclei (DAPI; blue). Scale bar 20  $\mu$ m.

Besides morphological properties, cell death can be visualized with marks that incorporate into the nucleus. We used apoptosis induced factor (AIF) as the marker of choice for identifying cellular death within the cortical culture. It was used in P6 culture fixed 24 hours post cut at DIV20. Under healthy conditions in the brain, AIF is located exclusively in the cytoplasm, specifically in mitochondria. Upon injury, if cells undergo apoptosis, AIF translocates to the nucleus<sup>47</sup>. 24 hours post cut, AIF positive nuclei were detected and counted at three randomized visual areas (AIF+;  $13.35 \pm 7.40$  %; n=187) near the cut site (Figure 19A, B). To confirm whether cells undergo apoptosis in areas far from the cut and in which cell types, AIF expression was tested in two randomized areas far from the cut for TUJ1+ neurons (Figure 19C, D) and vim+ astrocytes (Figure 19E, F) to see if it had localized to the nuclei. These cells were not counted, but the signal was found in nuclei for both neurons and astrocytes. The AIF signal had low expression and required a high exposure time. Therefore, this set



of experiments should be repeated and further analysed to validate the preliminary observations.

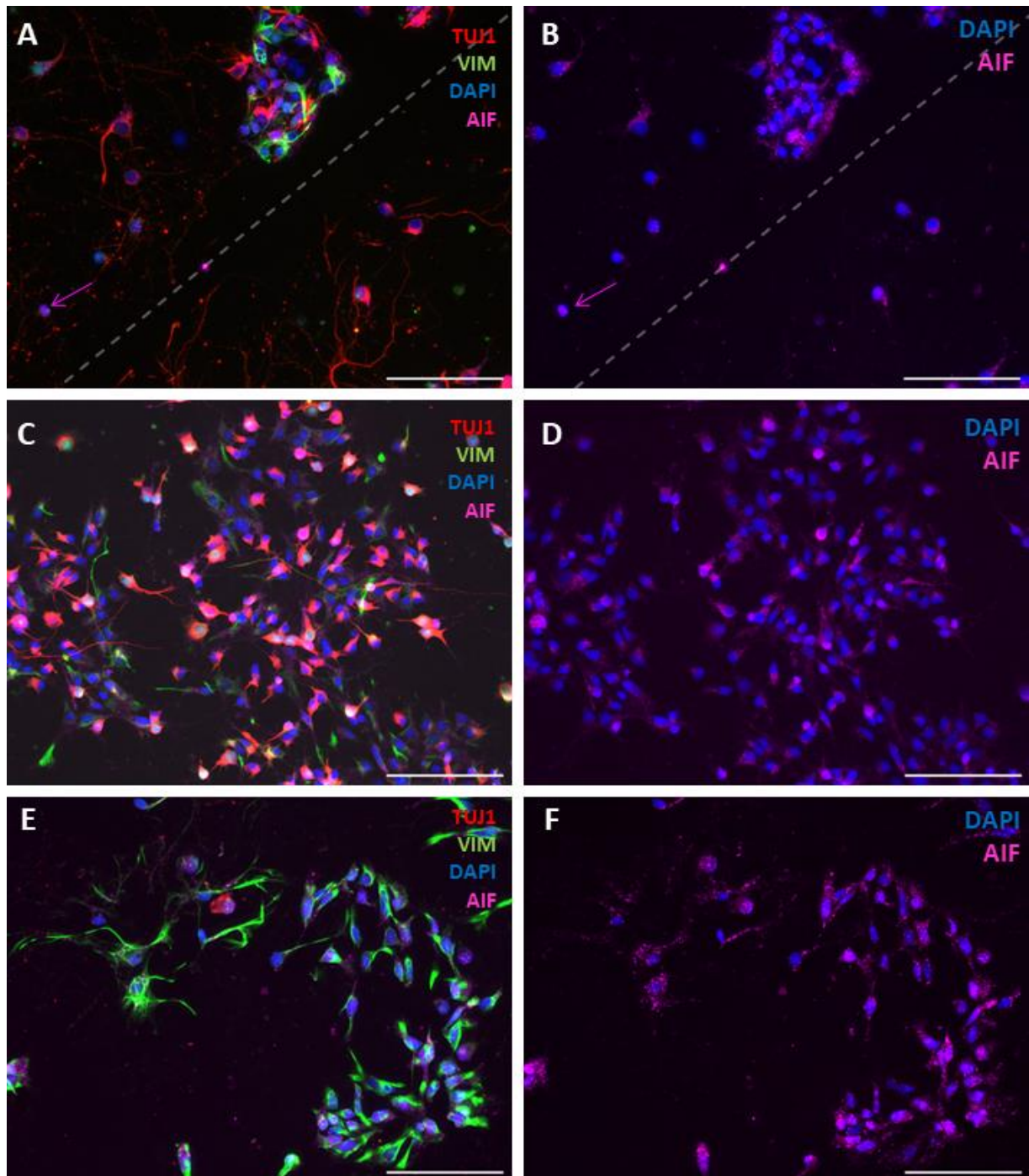


**Figure 19** P6 cortical culture fixed at DIV20, 24 hours post cut, and stained for  $\beta$ -tubulin III (TUJ1; red), vimentin (vim; green), nuclei (DAPI; blue), and apoptosis induced factor (AIF; magenta). **(A, B)** Cut site of the sample. Magenta arrows indicate a nucleus with colocalized DAPI and AIF signal. Dashed line represents the cut. **(C, D)** Control site for neurons far from the cut. **(E, F)** Control site for astrocytes far from the cut. Scale bar 100  $\mu$ m.

#### 4.3.2 Regeneration and glial scar formation in different *M. domestica* developmental ages

Cortical cultures prepared from different postnatal ages have different cell compositions and therefore it is expected that they could react differently to the injury. To investigate this response, two different comparisons were made: between the same developmental age but at different DIV, and between different developmental ages at the same DIV.

Firstly, cortical cultures of P6 opossums were analysed, one at DIV13 (Figure 20A), the other at DIV20 (Figure 20B). In both cases, cells were fixed 24 hours after the cut. Stronger vim signal is observed at DIV20 cortical culture, staining reactive astrocytes. These astrocytes seem to migrate across the cut junction, decreasing the injury size. Very few reactive astrocytes can be observed at DIV13. Neuronal density was comparable between the two samples. At DIV13, axons reach and sprout through the cut size, but at DIV20 neurons started forming connections through the cut. Higher neuronal connection number at DIV20 seem to occur in areas with less astrocytes, but this was not quantified.

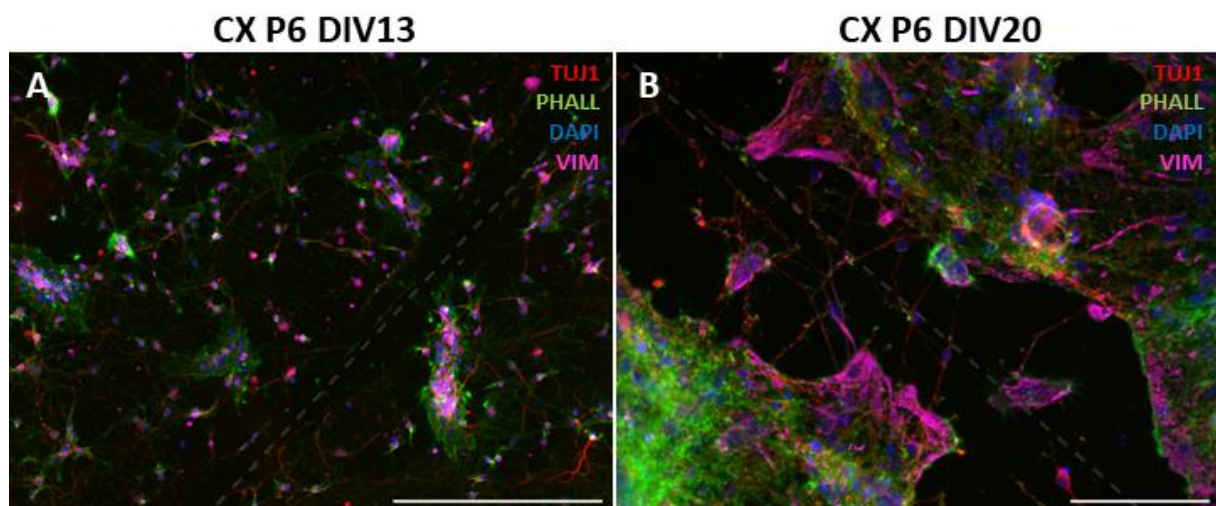


**Figure 20** Injury comparison between P6 cortical cultures fixed 24 hours after cut at **(A)** DIV13 and **(B)** DIV20. Samples were stained for  $\beta$ -tubulin III (TUJ1; red), filamentous (F) actin (PHALL; green), nuclei (DAPI; blue), and vimentin (vim; magenta). Dashed line represents cut site. Scale bar 200  $\mu$ m for DIV13 inset and 100  $\mu$ m for DIV20 inset. CX – cortex

Secondly, cortical cultures from P6 (Figure 21A) and P17 (Figure 21B) were compared. Both were cut and fixed after 24 hours at DIV13. P6 cortical cultures have a higher density of TUJ1+ neurons, in comparison with P17 cortical culture <sup>35</sup>. Consequently, a more extensive network of axons and neurites appears in P6 cultures, than in P17 culture at the cut site. Given that the vimentin staining wasn't entirely efficient, it is assumed that the TUJ1-negative cells with strong F-actin signal that migrated to the cut site in P17 cortical culture represent active astrocytes. Injury size reduction 24 hours after the cut is less evident in P6 cultures compared to P17 ones, again suggesting the active role of non-neuronal cells in cell response to injury.

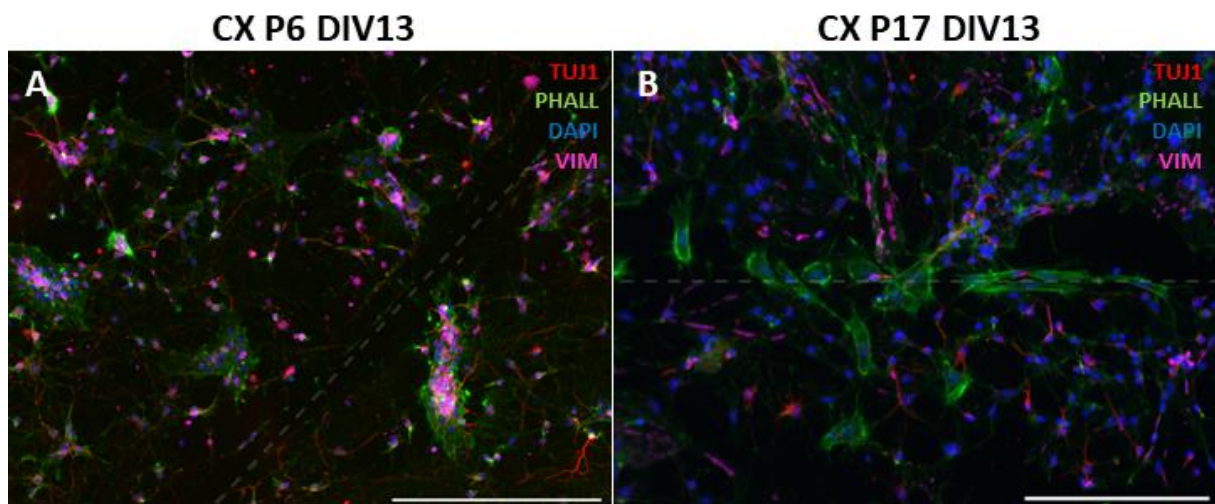


**Figure 21** Injury comparison between cortical cultures fixed 24 hours after cut at DIV13 in **(A)** P6 cortical culture and **(B)** P17 cortical culture. Sample was stained for  $\beta$ -tubulin III (TUJ1; red), filamentous (F) actin (PHALL; green), nuclei (DAPI; blue), and vimentin (vim; magenta). Dashed line represents cut site. Scale bar 200  $\mu$ m. CX – cortex.

#### 4.3.3 Growth cones versus retraction bulbs (following *in vitro* injury)

After traumatic injury, axonal elongation is possible. The ultimate fate of an extending axon at a cut site, whether it will survive or grow, can be observed through the formation of RBs and GCs (Figure 22A). GCs can be recognized by a strong, branched PHALL signal at the axonal terminus, with a formation of actin-rich filopodia and lamellipodia (Figure 22A, green



arrow). RBs also have a strong PHALL signal, but are morphologically different from GCs, as they form swellings at the tips of a growing axon, show disorganized microtubule organization and are associated with the loss of regenerative capacity after injury (Figure 22A, red arrow).

To check whether GCs change in size occurs 24 hours post cut at different *in vitro* maturation points, they were measured in cortical cultures derived from P6 opossums on two sets of samples fixed at DIV13 and DIV20. GCs at DIV13 are smaller ( $20.36 \pm 8.77 \mu\text{m}^2$ ,  $n=26$ ) than GCs at DIV20 ( $55.77 \pm 29.85 \mu\text{m}^2$ ,  $n=50$ ). These experiments should be repeated, however, given the high variability (SD) in the GCs size obtained. Is to be noted that neurons in culture are asynchronous and show different dynamics during neurite outgrowth and regeneration after *in vitro* injury which can result in different GC size inside the same sample.

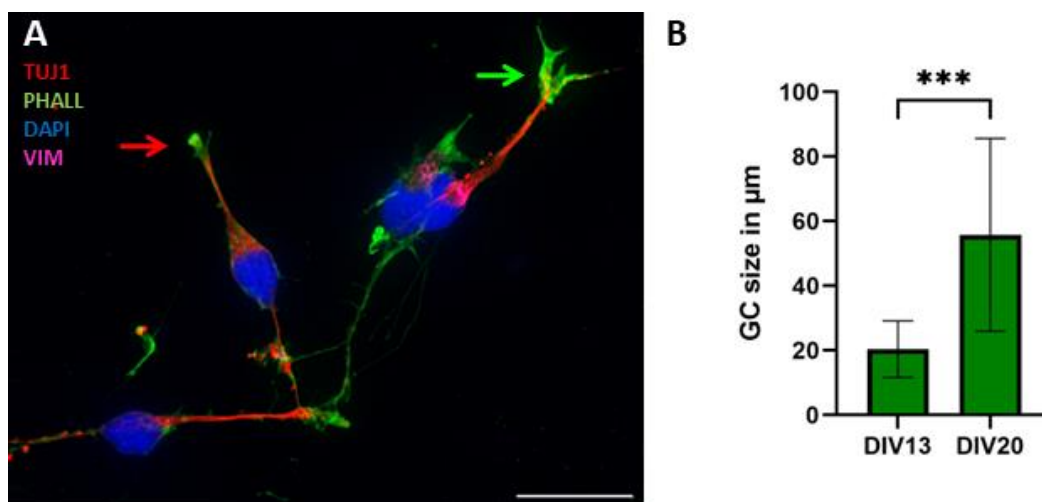


**Figure 22 (A)** P6 cortical culture at DIV20, fixed 24 hours post cut. Green arrow indicates a typical GC. Red arrow indicates a retraction bulb, swelling of axonal tip. Sample was stained for  $\beta$ -tubulin III (TUJ1; red), filamentous (F) actin (PHALL; green), nuclei (DAPI; blue), and vimentin (vim; magenta). Scale bar 20  $\mu\text{m}$ . **(B)** GCs are larger in DIV20 than in DIV13, 24 hours post cut. Unpaired *t*-test with Welch's correction. DIV13 vs. DIV20  $p < .001$  \*\*\*.

Regenerative potential of neuronal cultures declines with age. We have previously observed that cultures prepared from older opossums (P15-17) showed lower survival rate when compared to P3-5<sup>35</sup>. The reduced neuronal density and survival in P17 cultures resulted in an extremely limited number of GCs observed near the cut region.

## 5 DISCUSSION

The adult mammalian CNS remains incapable of regeneration after sustained injury. Moreover, its reduced ability to sprout injured neurons results in poor chances of recovery after injury <sup>48</sup>.

Development and regeneration of the CNS can be efficiently studied using *in vitro* primary cell cultures, as they're easier to handle compared to animals. Moreover, it's an ethically improved system which reduces the number of animals that are used, following the 3R principle: replacement, reduction, and refinement. In this case, *M. domestica* is the source animal for obtaining long-term primary neuronal cultures, given the advantages that they offer when using them as neuronal cell source. *M. domestica* neonates are born after a short gestation period of 14 days (1 week shorter than rodents) in their early developmental stage and have extended postnatal development of the CNS, with neurogenesis and gliogenesis reaching their peak and completing postnatally<sup>33,34</sup>. Additionally, dissociated cortical cells keep the ability to develop and became functional, and even regenerate *in vitro* for many weeks recapitulating many *in vivo* processes <sup>33</sup>. For comparison, regeneration after axotomy stops after 6 DIV for primary hippocampal E18 mice neurons <sup>49</sup>. Moreover, cortical cultures can be obtained at different developmental ages of young opossum pups, allowing the study of their different cellular composition through postnatal development, and their regenerative potential through their different developing phases. Therefore, successfully maintained cortical cultures derived from opossum pups offer additional advantages compared to rodents and provide a great insight into their distinct, age-dependent cellular composition changes, and their regenerative potential, as CNS injury can be performed and observed *in vitro*.

Primary neuronal cell cultures were obtained from cortexes of *M. domestica* following the protocol established by Petrović et al <sup>35</sup>. Two different ages of opossums were used in this thesis: P6 and P17. They

were maintained up to DIV20 for each developmental age. Through these 20 days it was possible to observe and characterize cellular composition of cultures, a change in cellular composition as they grew and matured, differentiation of neuronal and glial cells, cellular response to the injury, and regenerative potential. The majority of the work and developmental observations were made in P6 opossums, as P17 cultures were limited in numbers due to the lower cell density and survival observed at DIV20, not allowing comparison with other samples (for instance, DIV13 vs DIV20 GC size analysis, performed for P6 cultures).

Some of the observations made in P6 through different growth stages of cortical cultures include the cellular development of the cultures. Development was observed with the use of different neural and glial markers, in combination with F-actin stain, that was previously used only on P3-5 cultures at DIV1. In this work, F-actin allowed characterization of GCs after the cut (Figure 14 and 22), morphological characterization of astrocytes that form palisades at the lesion site (Figure 16 and 21) and perhaps the presence of oligodendrocytes (Figure 13 B and C).

TUJ1 was the main neural marker, a component of microtubular network that is specifically localized in dendrites and axons, as well as the cell body. It localises specifically in immature postmitotic neurons during the initial phases of neural differentiation. To further identify immature neurons, GAP-43 was used, while for mature neurons MAP2, a protein which is mostly localized in the soma and dendrites was effectively stained (Figure 11 and 13).

Glial development and composition were observed using vim, an intermediate filament protein found upregulated in developing as well as in reactive astrocytes. Vim is downregulated as astrocytes mature, resulting in upregulation of GFAP in mature astrocytes, a component of astrocytic cytoskeleton which helps define their shape and mobility <sup>41</sup>. To further identify astrocytes, S100 $\beta$  was used, a protein associated with cytoskeleton and membranes. Both of these are upregulated in activated

astrocytes as well. It is necessary to note that different vim antibodies were used in the following samples, a monoclonal rabbit IgG isotype and monoclonal mouse IgG<sub>1</sub> isotype, distinctive for their magenta or green fluorophores conjugated to different secondary antibodies used in these immunostained samples, respectively.

At DIV1, TUJ1 stained neuronal bodies started to develop, with their neurites sprouting and forming GCs at their tips, depicted by a strong PHALL signal. DIV1 cultures were abundant with immature neurons, accounting for 60% of all cells being TUJ1 positive, while vim positive cells accounted for 29% of cells. Surprisingly, 14% of cells expressed both TUJ1 and vim. In principle, these markers should be mutually exclusive<sup>50</sup>, with the reason of their mutual expression in cells being a possible result of antibody crosstalk, and markers not being completely specific for opossums. However, human fetal astrocytes were shown to co-express  $\beta$ -tubulin III together with vim and GFAP<sup>49</sup> which could support our observations. Other reason can be that at DIV1 vim is still not completely downregulated in cells that have begun their neuronal differentiation, upregulating TUJ1 (Figure 8A, red arrow; B and D, asterisk). Indeed, these cells show immature neuron morphology: short protrusions extending from soma instead of well-defined neurites observed in TUJ1+/vim- neurons. Their vim signal intensity was lower compared to the vim+/TUJ1-negative cells. Moreover, in this preparation, neuronal number was lower than in previous investigations in our laboratory where at DIV1 the majority of cells (>86%) of P3-5 cultures, expressed multiple neuronal markers: TUJ1, MAP2 and NeuN <sup>35</sup>. GAP43 staining and counting at DIV1 resulted in 56% of GAP43-positive cells, 52% of TUJ1-positive cells and 40% of double-positive cells within the culture. However, experiments conducted at DIV1 require additional experiments to validate them. Another additional control is required, using single immunostaining to ensure no antibody crosstalk occurs in our 4-color immunofluorescence experiment. This can be done using a different secondary antibody

conjugated with a different fluorophore (to check specificity of anti-rabbit 647 antibody), and possibly using an alternative GAP43 antibody. All these tests are required since, to our knowledge, GAP43 expression has not yet been investigated and validated by ICC in opossums.

At DIV5 of P6 cultures, axonal formation was detected, as well as neurite growth with sprouted GCs, with formation of first connections with neighbouring neurons, that in following days in culture formed an early neuronal network. At DIV 5 neuronal number increased very significantly (\*\*) in comparison with DIV1 cortical cultures, with TUJ1-positive cells accounting for 84% of cells, while vim-positive cell percentage significantly (\*) dropped to 17% of cells, with the presence of cells bearing the signal for both TUJ1 and vim markers at 11%. In comparison, Petrović et al. demonstrated that P3-5 cortical cultures were composed almost purely of neurons, accounting for >93% at DIV4, and non-neuronal percentage being stable at 2% <sup>35</sup>. The experimental difference observed here requires additional experiments to be performed.

At DIV13, neuronal number significantly (\*) decreased in comparison with DIV5, with neuronal cells accounting for 44%, and vim-positive cells accounting for 35%, indicating a change in cellular composition of cortical cultures through their development, i.e., the onset of gliogenesis *in vitro*.

Cell maturation was observed with multiple markers throughout development. In the early stages of development, specifically at DIV1 of P6 cultures, neurons were identified primarily with TUJ1, while GAP43 and MAP2 were used to determine different developmental stages of neurons. A similar approach was used to define astrocytic maturation, which was observed from DIV5 to DIV13 of P6 cortical cultures, through different signal expression between vim, an immature astrocyte marker and GFAP, a mature astrocyte marker. As expected, vim-positive cells at DIV5 were more numerous than GFAP-positive cells, accounting for 35% and 28%, respectively. The majority of GFAP-positive astrocytes co-expressed vim at 81%, indicating that vimentin expression precedes differentiation into

mature, GFAP positive astrocytes, with vimentin beginning its downregulation. At DIV13 two samples were immunostained, where GFAP was sampled with S100 $\beta$  (Figure 12B) and not with vim. Therefore, it's ratio with vim can only be compared with other, vim tested samples. They yielded similar percentages within cultures immunostained at DIV13, with vim remaining at 35% (n = 389) in one sample, and GFAP increasing to 32% (n = 267) of positive cells within its sample. Not only was cellular development of astrocytes observed, but also distinctive morphological features of mature astrocytes. Stellate and protoplasmic astrocytes were identified and best observed at DIV20 in P6 cortical cultures, when stained with monoclonal mouse vim antibody, yielding a much better signal than monoclonal rabbit antibody, depicting astrocytic intermediate filaments (Figure 12C, and D). This indicates that vim staining in these experiments could yield influenced data and results, requiring more experiments to be done in this experimental field. To further identify glial cells, Iba1 and NG2 were used as microglia<sup>44</sup> and oligodendrocyte<sup>41</sup> markers. Microglia presence was tested in both P6 and P17, at DIV13 and DIV20, respectively, while oligodendrocyte marker NG2 was used in P6 at DIV20, as gliogenesis occurs at later developmental phases<sup>34</sup>. While Iba1 yielded no signal, NG2 did, but it was not certain whether the signal is localized to a certain cell cytoplasm, so it was not further quantified (Figure 13A), as it requires more experiments as well.

The regenerative potential of cortical cultures was observed through the "scratch assay", an induced injury *in vitro*. Cultures were immunostained and fixed either 24 or 48 hours post cut in both age groups at different developmental phases.

Different neuronal and astrocytic reactions were induced by the injury. 24h post cut, we observed the presence of growing axons across the cut. At a certain proximity to the cut, they seem to change their growth direction, growing parallel to the, what is assumed, groove. As they extend, they also sprout GCs, if growth is successful, or RBs, which

ultimately halt their growth. Ultimately, they sprout across the cut to try forming connections with neighbouring axons. Astrocytes undergoing injury-induced astrogliosis have shown different responses depending on the culture age. In P6 cortical cultures fixed at DIV20 24h post cut, reactive astrocytes near the cut formed parallel palisades, with their elongated processes being polarized in the direction of the cut. These polarized processes contribute to the constitution of a barrier between the cut and the surrounding tissue and glial scar formation. In comparison, dormant astrocytes far from the cut remained “relaxed”, keeping their star-like shape. On the other hand, in P17 cortical cultures fixed at DIV13 also 24h post cut, astrocytes revealed migratory behaviour as they were localized at the cut site, with their cellular bodies expressing hypertrophic morphology. Given that vim staining wasn't fully successful, these cultures should be further investigated to confidently confirm cellular identity and define cellular morphological structures in depth.

Proliferation and cell death in injured cortical cultures were also observed. Proliferation was tested in P17 control and cut cortical cultures with EdU immunostaining. Expectedly, control cultures expressed higher EdU-stained cell percentage indicating proliferation, compared to the cut cultures. Cell death was tested in P6 cortical culture with AIF immunostaining. It was not quantified as it lacked a control counterpart, but it did show the presence of nuclei-localized AIF cells near the cut site. Dying cells within the cut site were also morphologically characterized by pyknotic nuclei within the cell and cellular blebbing.

Different regenerative processes were compared between different cortical culture development phases as well. When comparing two different cut cultures of the same P6 cultures, cut and fixed after 24h at DIV13 and DIV20, we observed higher regenerative potential of DIV20 cultures. While at DIV13, axons managed to begin sprouting through the cut, at DIV20 they already managed to form connections to the other side. Moreover, the gap size was reduced more at DIV20, given the induced

astrocyte reactivity to the injury, while at DIV13 little astrocytes were observed. When comparing P6 to P17 cultures at DIV13, less neurons were observed in P17, including less neurites and axons which grow through the cut. On the other hand, the cut size reduced more in P17 cultures, compared to P6 cultures.

The regenerative potential 24h after the cut at DIV13 and DIV20 using P6 cortical cultures was also tested using GC size analysis. GCs of DIV13 cultures showed an average size of around  $20 \mu\text{m}^2$ . Previous results obtained using P3-5 cortical cultures showed that the average GC size analysed at DIV1 was  $\sim 40 \mu\text{m}^2$ <sup>35</sup>. This observation suggests that more mature (DIV 13) neurons regrow smaller GCs 24h post cut compared to DIV1 neurons prepared from the same postnatal age. In contrast, experiments on DIV20 neurons gave higher GCs size ( $\sim 55 \mu\text{m}^2$ ). Given the high standard variation obtained, these results should be repeated. It would be interesting to verify if the increased presence of astrocytes at DIV20 compared to DIV13 (and their absence at DIV1) or changes in the composition of extracellular matrix over time, in addition to intrinsic neuronal regenerative potential, play a dominant role in the axonal outgrowth.



## 6 CONCLUSIONS

1. Primary cortical cultures derived from *M. domestica* are a great cell source to study neural cell development and regeneration of injury induced *in vitro* for extended period of time. In P6 cortical opossum cultures, 24h post injury, neurons extend their axons across the cut region, forming either growth cones or retraction bulbs, and this is possible to observe up to DIV20.
2. Opossum-derived primary cortical culture are mixed in composition: P6 are enriched with neurons (86% at DIV5) with progressively increased appearance of astrocytes in both P6 and P17 cultures. Opossum cortical astrocytes show similar expression pattern of intermediate filaments as observed in rodents and humans: vim is upregulated in immature astrocytes, co-express GFAP and downregulate vim during astrocyte maturation *in vitro*. Astrocytes had different responses in P6 and P17 cortical cultures 24h post cut. While in P6 cultures they assembled parallelly near the cut, polarizing their elongated processes and forming a barrier with the rest of the tissue, in P17 cortical cultures they migrated to the cut site. Our preliminary results show that proliferation (using EdU proliferation assay) as well as cell death (AIF staining) upon experimental injury can be investigated as well. Altogether, the coexistence of neurons and astrocytes resembles better the complex interplay of the tissue response after injury such as formation of glial scar. Further experiments could be performed to reveal the presence of microglia and oligodendrocytes as well and this could further increase the versatility and biological relevance of our cultures.
3. The regenerative potential differs between different developmental phases. In P6 cortical cultures, DIV20 neurons managed to form connections across the cut and had a stronger astrocyte response with reduced gap size, in contrast to DIV13 cortical cultures which only showed growing axons and little astrocytes near the cut. Furthermore, P17 cortical cultures had less neuronal activity induced by the cut than P6 cortical cultures at DIV13, but a more reduced cut size.

## 7 REFERENCES

- 1 Michael-Titus Adina, Revest Patricia, Shortland Peter. *Systems of The Body: The Nervous System - Basic Science and Clinical Conditions*. 2010<https://archive.org/details/nervoussystembas0002mich> (accessed 12 Jul2022).
- 2 Kandel ER, Koester JD, Mack SH, Siegelbaum SA. *Principles of Neural Science*. Sixth. McGraw Hill, 2012.
- 3 Haines DE, Gregory A, Mihailoff. *Fundamental Neuroscience for Basic and Clinical Applications*. 5th ed. 2017.
- 4 Salgado AJ. *Handbook of innovations in central nervous system regenerative medicine*. 2020.
- 5 Verkhratsky A, Parpura V. Introduction to Neuroglia. *Colloquium Series on Neuroglia in Biology and Medicine: From Physiology to Disease* 2014; **1**: 1–74.
- 6 von Bartheld CS, Bahney J, Herculano-Houzel S. The search for true numbers of neurons and glial cells in the human brain: A review of 150 years of cell counting. *Journal of Comparative Neurology* 2016; **524**: 3865–3895.
- 7 Cooper JA. Mechanisms of cell migration in the nervous system. *Journal of Cell Biology* 2013; **202**: 725–734.
- 8 Petros TJ, Tyson JA, Anderson SA. Pluripotent Stem Cells for the Study of CNS Development. *Front Mol Neurosci* 2011; **0**: 30.
- 9 Xu W, Lakshman N, Morshead CM. Building a central nervous system: The neural stem cell lineage revealed. *Neurogenesis* 2017; **4**: e1300037.
- 10 Martínez-Cerdeño V, Noctor SC. Neural progenitor cell terminology. *Front Neuroanat* 2018; **12**: 104.

- 11 Rakic P. Radial glial cells: Brain functions. *Encyclopedia of Neuroscience* 2009; : 15–21.
- 12 Mori T, Buffo A, Götz M. The Novel Roles of Glial Cells Revisited: The Contribution of Radial Glia and Astrocytes to Neurogenesis. *Curr Top Dev Biol* 2005; **69**: 67–99.
- 13 Marín O, Valiente M, Ge X, Tsai LH. Guiding neuronal cell migrations. *Cold Spring Harb Perspect Biol* 2010; **2**. doi:10.1101/CSHPERSPECT.A001834.
- 14 Tau GZ, Peterson BS. Normal development of brain circuits. *Neuropsychopharmacology* 2010; **35**: 147–168.
- 15 Jäkel S, Dimou L. Glial cells and their function in the adult brain: A journey through the history of their ablation. *Front Cell Neurosci* 2017; **11**. doi:10.3389/FNCEL.2017.00024.
- 16 Kim SU, de Vellis J. Microglia in health and disease. *J Neurosci Res* 2005; **81**: 302–313.
- 17 Ginhoux F, Prinz M. Origin of Microglia: Current Concepts and Past Controversies. *Cold Spring Harb Perspect Biol* 2015; **7**. doi:10.1101/CSHPERSPECT.A020537.
- 18 Kettenmann H, Ransom B. R. *The Concept of Neuroglia: A Historical Perspective*. Oxford: Oxford University Press, 2005.
- 19 Mahmoud S, Gharagozloo M, Simard C, Gris D. Astrocytes Maintain Glutamate Homeostasis in the CNS by Controlling the Balance between Glutamate Uptake and Release. *Cells* 2019; **8**. doi:10.3390/CELLS8020184.
- 20 Kimelberg HK, Nedergaard M. Functions of Astrocytes and their Potential As Therapeutic Targets. *Neurotherapeutics* 2010; **7**: 338–353.

- 21 Nave KA. Myelination and support of axonal integrity by glia. *Nature* 2010; **468**: 244–252.
- 22 Cameron HA, Glover LR. Adult neurogenesis: Beyond learning and memory\*. *Annu Rev Psychol* 2015; **66**: 53–81.
- 23 Emsley JG, Mitchell BD, Kempermann G, Macklis JD. Adult neurogenesis and repair of the adult CNS with neural progenitors, precursors, and stem cells. *Prog Neurobiol* 2005; **75**: 321–341.
- 24 Reynolds BA, Tetzlaff W, Weiss S. A multipotent EGF-responsive striatal embryonic progenitor cell produces neurons and astrocytes. *J Neurosci* 1992; **12**: 4565–4574.
- 25 Shoichet MS, Tate CC, Douglas Baumann M, LaPlaca MC. Strategies for Regeneration and Repair in the Injured Central Nervous System. *Indwelling Neural Implants: Strategies for Contending with the in Vivo Environment* 2008; : 221–244.
- 26 Hur EM, Saijilafu, Zhou FQ. Growing the growth cone: Remodeling the cytoskeleton to promote axon regeneration. *Trends Neurosci* 2012; **35**: 164–174.
- 27 Axon Regeneration And The Cytoskeleton. <https://www.cytoskeleton.com/axon-regeneration-and-the-cytoskeleton> (accessed 1 Aug2022).
- 28 Schiweck J, Eickholt BJ, Murk K, Bergami M, Reyes RC, de Britta KM *et al.* Important Shapeshifter: Mechanisms Allowing Astrocytes to Respond to the Changing Nervous System During Development, Injury and Disease. 2018. doi:10.3389/fncel.2018.00261.
- 29 Bardehle S, Krüger M, Buggenthin F, Schwausch J, Ninkovic J, Clevers H *et al.* Live imaging of astrocyte responses to acute injury reveals selective juxtavascular proliferation. *Nat Neurosci* 2013; **16**: 580–586.


- 30 VandeBerg JL, Robinson ES. The Laboratory Opossum ( *Monodelphis domestica* ) in Laboratory Research. *ILAR J* 1997; **38**: 4–12.
- 31 Cardoso-Moreira M, Halbert J, Valloton D, Velten B, Chen C, Shao Y *et al.* Gene expression across mammalian organ development. *Nature* 2019 571:7766 2019; **571**: 505–509.
- 32 Saunders NR, Adam E, Reader M, Møllgård K. *Monodelphis domestica* (grey short-tailed opossum): an accessible model for studies of early neocortical development. *Anat Embryol (Berl)* 1989; **180**: 227–236.
- 33 Nicholls JG, Stewart RR, Erulkar SD, Saunders NR. Reflexes, fictive respiration and cell division in the brain and spinal cord of the newborn opossum, *Monodelphis domestica*, isolated and maintained in vitro. *Journal of Experimental Biology* 1990; **152**: 1–15.
- 34 Puzzolo E, Mallamaci A. Cortico-cerebral histogenesis in the opossum *Monodelphis domestica*: Generation of a hexalaminar neocortex in the absence of a basal proliferative compartment. *Neural Dev* 2010; **5**: 1–18.
- 35 Petrović A, Ban J, Tomljanović I, Pongrac M, Ivaničić M, Mikašinović S *et al.* Establishment of Long-Term Primary Cortical Neuronal Cultures From Neonatal Opossum *Monodelphis domestica*. *Front Cell Neurosci* 2021; **15**. doi:10.3389/FNCEL.2021.661492/FULL.
- 36 Ban J, Mladinic M. *Monodelphis domestica*: A new source of mammalian primary neurons in vitro. *Neural Regen Res* 2022; **17**: 1726–1727.
- 37 Beta Tubulin III and neurogenesis. <https://www.novusbio.com//antibody-news/antibodies/beta-tubulin-iii-and-neurogenesis> (accessed 29 Aug2022).
- 38 O’Leary LA, Davoli MA, Belliveau C, Tanti A, Ma JC, Farmer WT *et al.* Characterization of Vimentin-Immunoreactive Astrocytes in the Human Brain. *Front Neuroanat* 2020; **14**: 31.


- 39 Holahan MR. GAP-43 in synaptic plasticity: molecular perspectives. *Res Rep Biochem* 2015; **5**: 137–146.
- 40 Carradori D, Eyer J, Saulnier P, Pr  at V, des Rieux A. The therapeutic contribution of nanomedicine to treat neurodegenerative diseases via neural stem cell differentiation. *Biomaterials* 2017; **123**: 77–91.
- 41 Bramanti V, Tomassoni D, Avitabile M, Amenta F, Avola R. Biomarkers of glial cell proliferation and differentiation in culture. *Front Biosci (Schol Ed)* 2010; **2**: 558–570.
- 42 Kiyatkin EA, Sharma HS. Environmental Conditions Modulate Neurotoxic Effects of Psychomotor Stimulant Drugs of Abuse. *Int Rev Neurobiol* 2012; **102**: 147–171.
- 43 Brozzi F, Arcuri C, Giambanco I, Donato R. S100B Protein Regulates Astrocyte Shape and Migration via Interaction with Src Kinase: IMPLICATIONS FOR ASTROCYTE DEVELOPMENT, ACTIVATION, AND TUMOR GROWTH. *J Biol Chem* 2009; **284**: 8797.
- 44 Microglia markers | Abcam. <https://www.abcam.com/neuroscience/microglia-markers> (accessed 29 Aug2022).
- 45 Petrovi   A, Ban J, Ivani  i   M, Tomljanovi   I, Mladinic M. The Role of ATF3 in Neuronal Differentiation and Development of Neuronal Networks in Opossum Postnatal Cortical Cultures. *Int J Mol Sci* 2022; **23**. doi:10.3390/IJMS23094964.
- 46 Kaiser CL, Kamien AJ, Shah PA, Chapman BJ, Cotanche DA. 5-Ethynyl-2'-deoxyuridine labeling detects proliferating cells in the regenerating avian cochlea. *Laryngoscope* 2009; **119**: 1770–1775.
- 47 Slemmer JE, Zhu C, Landshamer S, Trabold R, Grohm J, Ardeshiri A *et al*. Causal Role of Apoptosis-Inducing Factor for Neuronal Cell Death Following Traumatic Brain Injury. *Am J Pathol* 2008; **173**: 1795.

- 48 Tedeschi A, Omura T, Costigan M. CNS repair and axon regeneration: Using genetic variation to determine mechanisms. *Exp Neurol* 2017; **287**: 409–422.
- 49 Difato F, Tsushima H, Pesce M, Benfenati F, Blau A, Chierregatti E. The formation of actin waves during regeneration after axonal lesion is enhanced by BDNF. *Scientific Reports* 2011 1:1 2011; **1**: 1–10.
- 50 Butler R, Robertson J, Gallo J-M. Mutually exclusive expression of L III-tubulin and vimentin in adrenal cortex carcinoma SW13 cells. .

## PERSONAL INFORMATION

**Sara Mogorović**

 Pazin, Croatia

 (+385) 919227115

 [saramogorovic@gmail.com](mailto:saramogorovic@gmail.com) (primary); [sara.mogorovic@student.uniri.hr](mailto:sara.mogorovic@student.uniri.hr)

 Skype smogorovic

 LinkedIn <https://www.linkedin.com/in/saramogorovic/>

Sex Female | Date of birth 26<sup>th</sup> Sep, 1997 | Nationality Croatian

## EDUCATION AND TRAINING

Oct. 2019 – Sep. 2022	<b>Master of Science (MSc) in Drug Research and Development</b> <b>University of Rijeka, Department of Biotechnology</b> <b>Address:</b> Radmile Matejčić, 51000 Rijeka, Croatia <a href="http://www.biotech.uniri.hr/hr/">http://www.biotech.uniri.hr/hr/</a> Master thesis on topic "In vitro development and regeneration of primary cortical cell cultures of grey short-tailed opossum <i>Monodelphis domestica</i> ". Mentored by assoc. prof. Jelena Ban, PhD ( <a href="mailto:jelena.ban@uniri.hr">jelena.ban@uniri.hr</a> )	EQF LEVEL 7
Feb. 2020 - Jul. 2020	<b>Erasmus+ Student Exchange Program</b> <b>Autonomous University of Barcelona, Department of Biosciences and Biotechnology</b> <b>Address:</b> Plaça Cívica, 08193 Bellaterra, Barcelona, Spain <a href="http://www.uab.cat/">http://www.uab.cat/</a>	
Oct. 2016 - Sep. 2019	<b>Bachelor of Science (BSc) in Biotechnology and Drug Research</b> <b>University of Rijeka, Department of Biotechnology</b> <b>Address:</b> Radmile Matejčić, 51000 Rijeka, Croatia <a href="http://www.biotech.uniri.hr/hr/">http://www.biotech.uniri.hr/hr/</a>	EQF LEVEL 6
Sep. 2012 – May 2016	<b>High school graduate</b> <b>"Gymnasium and Vocational School Juraj Dobrila"</b> <b>Address:</b> Šetalište Pazinske Gimnazije 11, 52000 Pazin, Croatia <a href="https://www.gssjd.hr/">https://www.gssjd.hr/</a>	EQF LEVEL 4.2

## PROFESSIONAL EXPERIENCE

Oct. 2021 – Feb. 2022	<b>Member of Laboratory of Molecular Neurobiology</b> <b>Department of Biotechnology, Rijeka, Croatia</b> <a href="https://neuroreg.uniri.hr">https://neuroreg.uniri.hr</a> <b>Master Thesis Research Project</b> <b>Research topic:</b> <i>In vitro</i> cell development and regeneration during postnatal development of grey short-tailed opossum ( <i>Monodelphis domestica</i> ). <b>Techniques:</b> Work with cell cultures (neuronal, astrocyte), immunocytochemistry, light and fluorescence microscopy. Image analysis in CellSens (Olympus). Analysis and statistical data analysis: ImageJ/FIJI, GraphPad Prism	
-----------------------	--	--



Nov. 2019

### Student Assistant

Department of Biotechnology, Rijeka, Croatia

Student assistant for the course “Immunology”, supervised by Dr. sc. Ivana Munitić ([ivana.munitic@uniri.hr](mailto:ivana.munitic@uniri.hr))

**Role:** Introduction to laboratory practices used in aforementioned course, laboratory protocol walk-through and general student assistance.

Jul. 2019

### Professional practice - Research and Preformulation Department at JGL; Department of Public Health PGC

Jadran Galenski Laboratory (JGL), d.d. Svilno 20, Rijeka, Croatia

- First contact and introduction to the pharmaceutical industry: Dep. of Registration, Dep. of Research and Development, Quality Control, Production, Quality Assurance.

Department of Public Health PGC, Krešimirova 52a, Rijeka, Croatia

- First contact and introduction to the Department of Public Health: Dep. of Environmental Microbiology, Dep. of Control of Drinkable and Natural Waters, Dep. of Analytics.

## PERSONAL SKILLS

**Mother tongue(s)** Croatian

**Other language(s)**

	UNDERSTANDING		SPEAKING		WRITING
	Listening	Reading	Spoken interaction	Spoken production	
<b>English</b>	C2	C2	C1	C1	B2
OLS certificate					
<b>German</b>	A2	A2	A2	A2	A2
Self – Assessment					
<b>Italian</b>	B1	A2	B1	A2	A2
Self - Assessment					

Levels: A1/2: Basic user - B1/2: Independent user - C1/2 Proficient user  
Common European Framework of Reference for Languages

## Communication skills

Very good communication, disciplinal and teamwork skills acquired through:

- Oct 2016 – Sep 2022 - Laboratory practices as a Biotechnology student
- Jun 2016 – Sep 2022 - Student work (Waitress, Server, Shop Clerk)
- Feb 2020 – Jul 2020 - Erasmus+ Student exchange in Barcelona, Spain
- Oct 2021 – Current - Volunteering for Erasmus Student Network based in Rijeka, Croatia

**Computer skills**

- Advanced skills in Microsoft Office: Excel, Outlook, PowerPoint, and Word
- Basic skills in Adobe: Photoshop, Illustrator
- Basic skills in Data Analysis: GraphPad Prism, MedCalc, ImageJ
- Communication programs: Skype, Zoom, MS Teams
- Bioinformatics: VMD, PyMol, Chimera

**Laboratory skills**

- Gene cloning technique (PCR)
- Western blot
- Primary cell culture
- Immunocytochemistry
- Immunofluorescence and Light Microscopy

**Driving licence**

- AM, B

**ADDITIONAL INFORMATION**

---

**Volunteering**

- Erasmus Student Network (Rijeka, Oct. 2021 – Current)
- FORMA Association (Pazin, Mar. 2022 – Current)
- Student Association of Biotechnology (Rijeka, Oct. 2016 – Sep. 2022)
- Student mentor (Oct 2017 – Oct 2019)

**Competitions**

- STEM games competitor (Poreč, Croatia - 2018, 2019; Rovinj, Croatia - 2022)  
(<https://stemgames.hr/en/>)